

# Orthogonal Semiconductor: An exotic semiconductor of spinons

T. Farajollahpour<sup>1,2</sup> and S. A. Jafari<sup>2,3,\*</sup>

<sup>1</sup>*Department of Physics, Azarbaijan Shahid Madani University, 53714-161, Tabriz, Iran*

<sup>2</sup>*Department of Physics, Sharif University of Technology, Tehran 11155-9161, Iran*

<sup>3</sup>*Center of excellence for Complex Systems and Condensed Matter (CSCM), Sharif University of Technology, Tehran 1458889694, Iran*

We study the effect of strong correlations on the insulating state of a band insulator. In the absence of correlations the system is an insulator whose energy gap is determined solely by the gap parameter of the non-interacting theory. Upon increasing the Hubbard  $U$  at a critical point  $U_c^\perp$  where the rotor field disorders the quasi-particle weight  $Z$  of electron in both conduction and valence bands are lost, but still an Ising variable describing the charge fluctuations remains ordered. By further increase in  $U$  beyond  $U_c$  Ising field also disorders and the charge fluctuations are completely frozen resulting in a Mott state. The insulating state of system for  $U_c^\perp < U < U_c$  can be viewed as gapping an orthogonal metal by an staggered ionic potential. Such an orthogonal band insulating phase is characterized by temperature dependent band parameters arising from the temperature dependence of the underlying Ising order parameter. Furthermore optical gap is substantially smaller than the ARPES gap. Underlying Ising order provides extra sensitivity to external magnetic fields, and hence possible platforms for realization of orthogonal insulating states could include rare earth monochalcogenide semiconductors where the magneto-resistance is anomalously large.

PACS numbers: 72.20.-i, 71.27.+a, 71.30.+h

## INTRODUCTION

Strong short range interactions are an exciting paradigm for the emergence of non-Fermi liquid (NFL) behavior in low dimensional electron systems. As argued by N. Mott, strong Coulomb interactions can interrupt the conduction of electricity in an otherwise metallic state [1]. Since the proposal of Mott, the metal-to-insulator transition (MIT) has been investigated using various approaches [2]. The canonical model within which the MIT problem is investigated is the Hubbard model. Equally or even more interesting than the problem of MIT itself is the problem of possible exotic ground states when the interaction is not strong enough to stabilize a Mott insulating state, but is still strong enough to lead to exciting correlation induced phenomena. The list of possible methods to deal with the problem of strongly correlated systems and MIT includes but not limited to Gutzwiller approximation [3, 4], Strong coupling expansion [5–8], the Hubbard X operator methods [9], slave particle methods [10], slave rotor methods [11], slave spin methods [12, 13], exact diagonalization methods [14, 15], quantum Monte Carlo methods [16], path integral renormalization group [17], and dynamical mean field theory [18].

Strong correlation has its most profound effect on conducting states, i.e. metals by transforming them to a many-body insulating state. But this does not limit the attractiveness of strong correlations to metals only. Indeed as will be discussed in this study, the sensitivity of carrier concentrations of semiconductors to temperature can be utilized to distinguish correlation driven semiconducting transport from normal semiconductors. In the absence of tunability of the Hubbard  $U$  in solids, the correlated semiconductors may provide an exciting paradigm to search for possible signatures of spinons. Let us introduce the problem as follows: A Fermi gas can be

gapped out by adding a simple staggered electrostatic potential of strength  $\Delta$  that creates Bragg reflections at the Brillouin zone boundaries. When the short range interactions are turned on in such an already gapped state (band insulator) an interesting competition between the Hubbard  $U$  and the staggered potential  $\Delta$  sets in. The simple model addressing the competition between a "many-body" gap parameter  $U$  and a "single-particle" gap parameter  $\Delta$  is the so called ionic Hubbard model [19]. This model is an extension of the Hubbard model where a staggered electrostatic potential characterized by an energy scale of  $\Delta$  (the so called ionic potential) gives rise to a band insulating state in the  $U = 0$  limit. This state is adiabatically connected to non-zero but small values of  $U \ll \Delta$  as the effect of Hubbard  $U$  is to renormalize the "parent" metallic state on top of which the ionic potential creates a band insulator (BI) state. In the opposite limit of strong correlations  $U \gg \Delta$  one gets a Mott insulating (MI) state. Although these two extreme limits both represent insulating states, the nature of gap in the former case is a simple one-particle scattering, while in the later case it has a many-body character.

The nature of possible state(s) between the above two extreme insulating states has been the subject of debates in the past decade. In one dimension Fabrizio and coworkers [20] find an ordered state. In two dimensions Hafez-Torbati and coworkers find orientational and bond ordering phase in between the Mott and band insulators [21]. The topologically non-trivial variant of the model was considered by Prychynenko and coworkers [22] who find for topologically trivial situation two spin density wave states are sandwiched between the band and Mott insulating states. In the limit of infinite dimensions Garg and coworkers using the dynamical mean field theory found that the competition between the tendency of the ionic potential  $\Delta$  and the Hubbard term  $U$  gives rise to a metallic state [23]. Within a perturbative con-

tinuous unitary transformation also one finds a metallic state when the Hubbard  $U$  and the ionic potential  $\Delta$  are comparable [24]. Similar result were obtained in two dimension [25]. The method of dynamical mean field theory was also applied to study the quantum phase transitions of the ionic Hubbard model on the honeycomb lattice. Starting from massive Dirac fermions on the honeycomb lattice the competition between  $U$  and the single-particle gap parameter  $\Delta$  (known as mass term when it comes to Dirac fermions) gives rise to massless Dirac fermions [26]. A recent strong coupling expansion gives a quantum critical semi-metallic state [7].

The problem of strongly correlated band-insulator or semiconductor can also be viewed from another interesting angle: Nandkishore and coworkers have argued that starting from a metallic state, as one increases the Hubbard  $U$  beyond  $U_c^\perp$  the Fermi liquid (FL) undergoes a phase transition to an exotic state termed orthogonal metal (OM). Upon further increase in the interaction strength beyond  $U_c$  the system becomes a Mott insulator [27]. OM is an exciting – and perhaps the simplest – non-Fermi liquid state for  $U_c^\perp < U < U_c$  that separates a FL from a Mott insulator. This state is characterized by condensation of a two-charge object. This can be technically captured within the slave-spin method where an Ising order parameter is accompanied by spinons responsible for the transport. Even within the mean field approximation, the *enslaved* Ising order parameter serves to provide sensitivity to temperature and external magnetic fields. This idea as will be discussed in detail when imported from a metal to a semiconducting state gives rise to an exotic semiconductor made of spinons. When an OM state is probed with angular resolved photoemission spectroscopy (ARPES) due to vanishing of the quasiparticle weight of the physical electron a gap is seen by ARPES. But since the Fermi surface of spinons survives due to a non-zero Ising order parameter, the quantum oscillations experiment will find a Fermi surface [28].

In the FL phase the rotor variable is ordered, i.e. the phase variable has small fluctuations meaning that the electric charge has large fluctuations. When the rotor variable disorders, old interpretation would assume that wild fluctuations of the rotor field corresponds to freezing of charge fluctuations, thereby making the system a Mott insulator [11]. However, Nandkishore and coworkers argued that even if the rotor variable is disordered, i.e.  $\langle e^{i\theta} \rangle = 0$ , and a single boson  $b \sim e^{i\theta}$  is not condensed, a two-boson combination can still be condensed,  $\langle bb \rangle \neq 0$ . This can be naturally captured within a slave spin approach [12] where the condensation of two-boson combination is reflected in a non-zero Ising order parameter. In this OM state although the quasiparticle weight corresponding to physical electrons is zero, its transport behavior is metallic. To see this, the following simple and powerful argument is due to Nandkishore and coworkers: Within the slave spin representation the physical electron is represented as  $c_\sigma^\dagger = f_\sigma^\dagger \tau^x$ . The  $U(1)$  gauge freedom representing the conservation of the electric (Noether) charge can only be incorporated into the spinon  $f_\sigma^\dagger$  as the Pauli matrix  $\tau^x$  is purely real. Therefore the  $f$  spinons inherit the whole charge

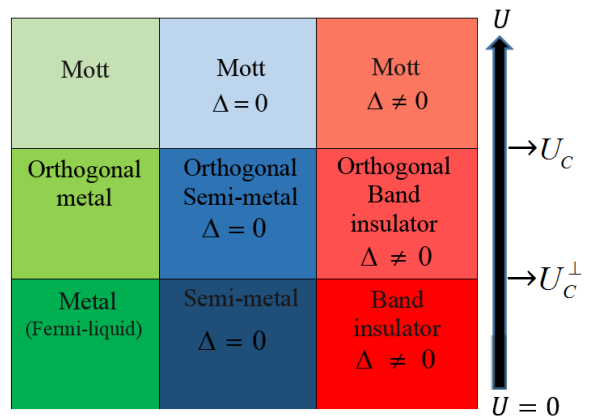


FIG. 1. (Color online) The schematic representation of the effect of correlation on three starting states. The non-interacting state from which we start is drawn in the bottom row. Left column corresponds to metallic state, middle column stands for semi-metallic state and the right column denotes the band insulating state. All columns at very large  $U$  end in the Mott insulating states (top row). The middle row is the corresponding "orthogonal" phase where the transport is controlled by the spinons that inherit the charge of the original electrons.

from the parent electrons and after the rotor disordering transition the spinons will continue to display metallic transport properties despite that the quasiparticle weight of the physical electrons has already vanished at  $U_c^\perp$ . If instead of a metallic state at  $U = 0$ , one starts with a semi-metallic state (such as graphene) the state bounded by the disordering transition of rotors and Ising spins would give rise to an orthogonal semi-metal [29].

Our discussion so far is schematically summarized in the first two columns of Fig. 1. Let us now get back to the question of possible phases of the ionic Hubbard model. In the bottom row in Fig. 1 one possible state at  $U = 0$  is a simple Metal. The second possibility is the semi-metal. The third possibility is a band insulator (semiconductor) that can be simply generated from the first column by adding a staggered ionic potential. In this table the upper row is always a Mott state born out of various states at the bottom row. The middle row corresponding to  $U_c^\perp < U < U_c$  is the exotic orthogonal phase. Motivated by the mentioned debates on the fate of the competition between the Hubbard  $U$  and the ionic potential  $\Delta$ , and in the light of the exciting possibility of an "orthogonal" phase schematically depicted in Fig. 1, in this work we study the ionic Hubbard model on the honeycomb lattice within the slave rotor and slave spin representations with their associated disordering quantum transitions. The general picture that emerges is as follows: At small values of Hubbard  $U$  the gapped state is adiabatically connected to a band insulator. At a first critical value  $U_c^\perp$  the disordering transition of the underlying enslaved rotor variables leaves the states in both conduction and valence bands inaccessible to ARPES, while accessible to any probe coupling to the electric current, such as optical conductivity, cyclotron resonance and thermal probes.

This will play a significant role in experimental discrimination of insulators (semiconductors) from their orthogonal relatives. At a second (higher) critical value  $U_c$  the underlying slaved Ising variable also disorders and the system ends in the Mott insulating state. The phase between the Mott and band insulating state can be named orthogonal band insulator (OBI). Possible systems to search for indications of such an unusual insulating state would include rare earth monochalcogenides where the resistance displays high sensitivity to applied magnetic fields. This could be due to the coupling of applied field to the condensate of Ising variables. The results of this paper applies to a quite general correlated insulators. However in this paper we focus on honeycomb system where the parent band insulator is described by massive Dirac electrons [34].

This paper is organized as follows: In section II after introducing the ionic Hubbard model, we review the slave-rotor method and customize it for the ionic Hubbard model. In section III we adopt the version of slave-spin employed in [12]. Based on symmetry principles we discuss under what circumstances the Lagrange multiplier implementing the constraint between Ising spin and spinon degrees of freedom vanishes. In section IV we discuss the results and summarize the findings at the end.

## IONIC HUBBARD MODEL AND SLAVE ROTOR METHOD

We are interested in the phase diagram of the Hubbard model augmented by an staggered ionic potential of strength  $\Delta$  as follows:

$$H = H_0 + \frac{U}{2} \sum_i (n_{i\uparrow} + n_{i\downarrow} - 1)^2 \quad (1)$$

$$H_0 = -t \sum_{\langle i,j \rangle \sigma} c_{i\sigma}^\dagger c_{j\sigma} + \Delta \sum_{i\sigma} (-1)^i n_{i\sigma} - \mu \sum_{i\sigma} n_{i\sigma} \quad (2)$$

where  $c_{i\sigma}^\dagger$  creates an electron at a localized orbital in site  $i$  with spin  $\sigma$ ,  $n_{i\sigma} = c_{i\sigma}^\dagger c_{i\sigma}$  is the occupation number,  $U$  is the on-site Hubbard repulsion,  $t$  is the hopping amplitude which will be set as the unit of energy through out the paper,  $\Delta$  is the ionic potential, and  $\mu$  is the chemical potential that at half-filling in the present representation turns out to be  $\mu = 0$ .

### Slave rotor method

The slave rotor formulation is one of the slave particle family methods employed in the studying the Hubbard model that provides a very economical representation of the charge state of an orbital in terms of a rotor variable conjugate to an angular momentum operator that itself is locked to the charge [11]. This method can also be applied to the study of Anderson impurity problem [30]. In this approach the local Hilbert space is represented by a direct product of the Hilbert space of a fermion carrying the spin index (the so called spinon) and a rotor that controls the charge state of the system as

$|\psi\rangle = |\psi_f\rangle |\psi_\theta\rangle$ . In terms of operator creating a particle from its vacuum the above equation can be represented as,

$$\hat{c}_{i\sigma}^\dagger = f_{i\sigma}^\dagger e^{-i\theta_i}, \quad (3)$$

where  $f_{i\sigma}^\dagger$  is the spinon creation operator and  $\theta_i$  is the rotor variable at site  $i$ . The physical Hilbert space of the electron in terms of the spinons and rotors are given as follows:

$$\begin{aligned} |0\rangle &\equiv |0\rangle_f |-1\rangle_\theta \\ |\uparrow\rangle &\equiv |\uparrow\rangle_f |0\rangle_\theta \\ |\downarrow\rangle &\equiv |\downarrow\rangle_f |0\rangle_\theta \\ |\uparrow\downarrow\rangle &\equiv |\uparrow\downarrow\rangle_f |1\rangle_\theta \end{aligned} \quad (4)$$

where  $|L\rangle_\theta$  represents an state in the rotor space, and  $|a\rangle_f$  represents a possible state in the spinon Hilbert space. As can be seen in the above representation states such as  $|\uparrow\rangle_f |-1\rangle_\theta$  containing one  $\uparrow$ -spin spinon and corresponding to angular momentum eigen state of  $-1$  does not correspond to any physical state. Such redundancy is a characteristic of auxiliary particle methods where the physical Hilbert space is enormously enlarged. What we gain in the enlarged Hilbert space is the gauge freedom. But the physically sensible state are obtained from those in the enlarged space by projecting them to the physical space. In the present case such a projection amounts to the constraint

$$\sum_\sigma f_{i\sigma}^\dagger f_{i\sigma} = L_i + 1 \quad (5)$$

It can be checked that all of the states in Eq. (4) satisfy the above constraint. If the above constraint can be implemented exactly, then either of the representation in terms of original electrons or in terms of spinons and rotors give identical result. But the full-fledged implementation of the above projection requires to fully take the gauge fluctuations into account. In the present work we treat the constraint in the mean field via an space- and time-independent Lagrange multiplier. This is known as the slave rotor mean field approximation [11, 31].

Let us proceed with representing the electron operators in terms of spinons and rotors, Eq.(3),

$$\begin{aligned} H = & - \sum_{\langle ij \rangle, \sigma} f_{i\sigma}^\dagger f_{j\sigma} e^{-i\theta_{ij}} + \text{h.c.} + \Delta \sum_i f_i^\dagger f_i - \Delta \sum_j f_j^\dagger f_j \\ & + \frac{U}{2} \sum_i L_i^2 - \mu \sum_{i\sigma} f_{i\sigma}^\dagger f_{i\sigma} + h \sum_i \left( f_{i\sigma}^\dagger f_{i\sigma} - L - 1 \right), \end{aligned} \quad (6)$$

where the hopping amplitude  $t$  of original electrons is set as the unit of energy,  $t = 1$ ,  $\theta_{ij} = \theta_i - \theta_j$ , the Hubbard term of Eq. (1) has been transformed with the aid of the constraint (5),  $\mu$  is the chemical potential that becomes zero at half-filling which is our focus in this paper, and  $h$  is a position-independent Lagrange multiplier that implements the constraint (5) on average. The merit of representation in terms of auxiliary rotor variables is that the quartic interaction between the fermions  $U/2 \sum_{i\sigma} (n_{i\sigma} - 1)^2$  is replaced by

a simple kinetic term  $UL^2/2$  at every site, where the angular momentum  $L = -i\partial_\theta$  is a variable that is associated with a  $O(2)$  quantum rotor  $\theta$ .

Apart from the kinetic term that combines spinons and rotors on neighboring sites, the above Hamiltonian is decoupled into a rotor ( $\theta$ -only), and spinon ( $f$ -only) terms. As for the first term we introduce mean field variables,

$$\chi_\theta = \langle e^{i\theta_i} e^{-i\theta_j} \rangle_\theta, \quad (7)$$

$$\chi_f = \left\langle \sum_\sigma f_{\sigma i}^\dagger f_{\sigma j} \right\rangle_f, \quad (8)$$

to decouple the kinetic term, which eventually gives decoupled rotor,  $H_\theta$  and spinon  $H_f$  Hamiltonians

$$\begin{aligned} H_f = & - \sum_{\langle ij \rangle, \sigma} f_{i\sigma}^\dagger f_{j\sigma} \chi_\theta + \text{h.c.} + (\lambda - \mu) \sum_{j\sigma} f_{j\sigma}^\dagger f_{j\sigma} \\ & + \Delta \sum_{i \in A} f_{i\sigma}^\dagger f_{i\sigma} - \Delta \sum_{j \in B} f_{j\sigma}^\dagger f_{j\sigma}, \end{aligned} \quad (9)$$

and

$$H_\theta = \sum_{\langle i, j \rangle} \chi_f e^{i\theta_i - i\theta_j} + \text{h.c.} + \sum_j \left( \frac{U}{2} L_j^2 - \lambda L_j \right), \quad (10)$$

where  $A$  and  $B$  are the two sub-lattices on the honeycomb lattice. In the above equation, solution of the  $H_f$  requires a knowledge of  $\chi_\theta$  which according to Eq. (7) can only be calculated after having diagonalized the rotor sector  $H_\theta$ . The later itself depends on unknown quantity  $\chi_f$  that according to Eq. (8) can be obtained from the  $H_f$  Hamiltonian. This provides a self-consistency loop, i.e. the rotor and the spinon sectors talk to each other via the mean-field self-consistency equations, (7) and (8).

It is interesting to note that in Eq. (9) the ionic potential  $\Delta$ , being a local potential couples only to the spinon density. This considerably simplifies the analysis of the problem. Indeed in the absence of ionic potential  $\Delta$ , the spinon sector would have been described by spinon hopping Hamiltonian with renormalized hopping amplitudes whose reduced kinetic energy is encoded in  $\chi_\theta$  self-consistently determined by the rotor sector. When the ionic potential is turned on, the spinon sector describes spinons hopping with renormalized hopping parameters  $\chi_\theta$ , plus an additional Bragg reflection due to doubling of the unit cell that always gaps out the spinon sector and the spectrum in the spinon-sector is given by,

$$\varepsilon_f(\vec{k}) = \pm \sqrt{\chi_\theta^2 |\phi(\vec{k})|^2 + \Delta^2} \quad (11)$$

where  $\phi(\vec{k}) = 1 + e^{i\vec{k} \cdot \vec{a}_1} + e^{i\vec{k} \cdot \vec{a}_2}$  with  $\vec{a}_1$  and  $\vec{a}_2$  unit being translation vectors of the honeycomb lattice.

Now let us turn to determination of chemical potential  $\mu$  and Lagrange multiplier field  $\lambda$ . Since we are interested in the competition between  $U$  and  $\Delta$ , we stay at half-filling where even in the  $U = 0$  limit the system is described by a simple band insulator. The particle-hole symmetry of the original Hamiltonian in terms of physical electrons simply implies that

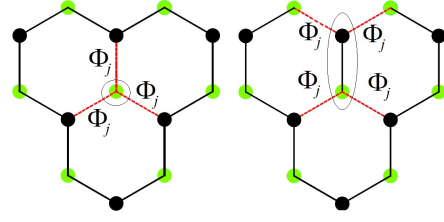


FIG. 2. (Color online): Two possible clusters for the solution of the slave rotor. The dotted lines indicate the mean field value of the rotor field connecting the cluster at hand to its neighbors.

at half-filling  $\mu = 0$ . Since we want to fix the average occupation at  $n = 1$ , the constraint (5) implies that on average one should have  $\langle L_j \rangle = 0$  for every lattice site  $j$ . Now imagine that in a rotor Hilbert space corresponding to a given total angular momentum  $\ell$ , we construct the local angular momentum operator  $UL_j^2/2 - hL_j$  that would take  $2\ell + 1$  diagonal values  $U(n_j^\theta)^2 - \lambda n_j^\theta$ , where  $n_j^\theta = -\ell \dots \ell$  represents all possible values of the magnetic quantum number. Obviously any non-zero value of  $\lambda$  breaks the symmetry between the states corresponding to positive and negative values of  $n_j^\theta$  and therefore makes the expectation value  $\langle L_j \rangle$  non-zero that places us away from half-filling. Therefore at half-filling an emergent *time-reversal symmetry* pins down the Lagrange multiplier  $\lambda$  to zero.

Now the remaining challenge is to solve the rotor problem posed by the Hamiltonian (10). One simple way to think of the rotor Hamiltonian is to fix a value for  $\ell$  that gives a local dimension of  $2\ell + 1$  for each rotor. This Hilbert space grows as  $N^{2\ell+1}$  where  $N$  is the number of lattice sites. However if we further decouple the two-site terms as

$$e^{-i\theta_i - i\theta_j} \approx e^{-i\theta_i} \langle e^{i\theta_j} \rangle + \text{h.c.} = e^{-i\theta_i} \Phi_j + \text{h.c.}, \quad (12)$$

where a mean field rotor variable  $\Phi_j = \langle e^{i\theta_j} \rangle$  is introduced, the rotor problem is considerably simplified. This mean field decomposition can be implemented on various clusters. We consider two types of clusters with finite number of sites denoted in Fig. 2. For the single-site cluster the mean field variables connect the given site to its neighbors on the lattice, and the single-site Hamiltonian has no structure. In this case the mean field rotor Hamiltonian for every site is given by,

$$H_\theta^{1\text{-site MF}} = -3\chi_f \Phi (e^{-i\theta} + e^{i\theta}) + \frac{U}{2} (n^\theta)^2 \quad (13)$$

where the coefficient of 3 is due to three neighbors of every single-site (Fig. 2, left side). The explicit matrix representation of the above single-site mean field Hamiltonian is,

$$\begin{bmatrix} u\ell^2 & -3\chi_f \Phi & 0 & \dots & 0 \\ -3\chi_f \Phi^* & u(\ell-1)^2 & -3\chi_f \Phi & \dots & 0 \\ 0 & -3\chi_f \Phi^* & \ddots & \dots & \vdots \\ \vdots & \vdots & -3\chi_f \Phi^* & u(-\ell+1)^2 & -3\chi_f \Phi \\ 0 & 0 & \dots & -3\chi_f \Phi^* & u(-\ell)^2 \end{bmatrix} \quad (14)$$

where for notational brevity we have introduced  $u = U/2$ . Within the mean field a two-site cluster can also be adopted (see Fig. 2) for which the Hamiltonian becomes

$$H_{\theta}^{2\text{-site MF}} = -\chi_f (e^{-i\theta_1} e^{i\theta_2} + e^{-i\theta_2} e^{i\theta_1}) - 4\chi_f \Phi (\cos \theta_1 + \cos \theta_2) + u(n_1^\theta)^2 + u(n_2^\theta)^2 \quad (15)$$

The above Hamiltonian operates in the two-particle space represented by  $|n_1^\theta, n_2^\theta\rangle$  where  $n_i^\theta = -\ell_i \dots \ell_i$  for  $i = 1, 2$ . The effect of the two-site MF Hamiltonian on every such state is given by

$$\begin{aligned} & -\chi_f (|n_1^\theta - 1, n_2^\theta + 1\rangle + |n_1^\theta - 1, n_2^\theta + 1\rangle) \\ & - 2\chi_f \Phi \sum_{a=\pm 1} (|n_1^\theta + a, n_2^\theta\rangle + |n_1^\theta, n_2^\theta + a\rangle) \\ & + u (n_1^{\theta 2} + n_2^{\theta 2}) |n_1^\theta, n_2^\theta\rangle \end{aligned} \quad (16)$$

The following algorithm self-consistently determines all the mean field parameters: For given set of external parameters such as  $U$ , (I) Start with an initial guess for  $\chi_f$ . (II-a) For the above  $\chi_f$ , guess a  $\Phi$ . (II-b) Diagonalize the matrix (14) and obtain its ground state. (II-c) In the obtained ground state update the  $\Phi = \langle e^{i\theta} \rangle$  and keep repeating until  $\Phi$  is self-consistently determined. (III) For the present value of  $\chi_f$  and  $\Phi$ , use Eq. (7) to obtain  $\chi_\theta$ . (IV) Plug in the  $\chi_\theta$  into the spinon Hamiltonian (9) and diagonalize it. (V) For the ground state of the above spinon Hamiltonian use Eq. (8) to update the initial guess  $\chi_f$ . This procedure is repeated until mean field parameters  $\chi_f, \chi_\theta, \Phi$  are self-consistently determined. It must be noted that the above procedure is done for a fixed value of  $\ell$ . One has to keep increasing  $\ell$  to ensure that the final converged results do not change much upon further increase in the dimension of the rotor space. We confirm that  $\ell = 2$  is accurate enough [31].

Upon increasing the Hubbard interaction  $U$  beyond a critical point the mean field parameter  $\Phi$  vanishes that corresponds to strong fluctuations in the phase variable, and hence frozen fluctuations of the corresponding number operators, i.e. *putative* Mott state.

### SLAVE SPIN METHOD

The charge degree of freedom at every site can be described by variety of methods. Description in terms of a rotor variable whose conjugate variable controls the charge state is one possibility. Another appealing possibility is to use an Ising variable to denote the charge state. Using an Ising variable to specify the electric charge can be implemented in various ways [12, 13, 32]. In this section we briefly review the presentation of Ref. [12] and adopt it in our investigation of the ionic Hubbard model on the honeycomb lattice.

In this representation an Ising variable  $\tau$  is introduced to take care of the charge configuration of every site. Empty and double occupied configuration are represented by  $|+\rangle$ , while

those with a local moment both are represented by  $|-\rangle$  defined by

$$\tau^z |\pm\rangle = (\pm 1) |\pm\rangle \quad (17)$$

The correspondence between physical states and those in the Hilbert space extended by introduction of Ising variables is:

$$\begin{aligned} |\text{empty}\rangle &= |+\rangle |0\rangle \\ |\text{singly occupied, } \uparrow\rangle &= |-\rangle |\uparrow\rangle \\ |\text{singly occupied, } \downarrow\rangle &= |-\rangle |\downarrow\rangle \\ |\text{doubly occupied}\rangle &= |+\rangle |\uparrow\downarrow\rangle. \end{aligned} \quad (18)$$

where states on the left hand correspond to physical electrons, and those in the right hand are product of states corresponding to Ising variables,  $|\pm\rangle$ , and those corresponding to spinon. Creation of each electron has almost a parallel on the right side implying that  $c^\dagger \sim f^\dagger$ . However each time an electron is created, the charge state flips between the one having a local moment and those having no local moment. This corresponds to a flip in the Ising variable that can be achieved with the action of Pauli matrix  $\tau^x$ . Therefore the physical electron at every site  $j$  can be represented as,

$$c_{j\sigma}^\dagger \equiv \tau_j^x f_{j\sigma}^\dagger. \quad (19)$$

where  $f_{j\sigma}^\dagger$  creates a spinon of spin  $\sigma$  at site  $j$ . The fact that creation of each physical charge is synonymous to creation of an spinon implies that the physical charge is basically carried by spinons. This was a key observation made by Nandkishore and coworkers [28] that is formally reflected in Eq. (19) as the fact that the Pauli matrix  $\tau^x$  being a real matrix can not absorb the  $U(1)$  charge, and hence all the charge of electron is carried by the spinons.

The Hilbert space represented by the product of Ising and spinon spaces is huge and includes states such as  $|+\rangle |\uparrow\rangle$ , etc do not correspond to any physical state. Inspection shows that those states can be eliminated by the following constraint:

$$\tau_j^z + 1 - 2(n_j - 1)^2 = 0. \quad (20)$$

In this new representation the ionic Hubbard Hamiltonian becomes,

$$\begin{aligned} H &= - \sum_{\langle ij \rangle} \tau_i^x \tau_j^x f_{i\sigma}^\dagger f_{j\sigma} + \frac{U}{4} \sum_j (\tau_j^z + 1) \\ &+ \Delta \sum_j f_{j\sigma}^\dagger f_{j\sigma} (-1)^j \end{aligned} \quad (21)$$

where as before the hopping  $t$  of the physical electrons is set as the unit of energy and the constraint Eq. (20) has enabled us to cast the Hubbard  $U$  into a form involving only Ising variable  $\tau^z$ . Again in the ionic potential term the Ising spins being squared to unit matrix cancel each other and hence the staggered ionic potential is only coupled to the spinons. Mean-field decoupling of the Ising and spinon variables is lead to

two separate Hamiltonians governing the dynamics of spinons  $f$  and Ising variables  $\tau$  as follows:

$$H_f = - \sum_{ij} \chi_I f_{i\sigma}^\dagger f_{j\sigma} + \Delta \sum_j f_{j\sigma}^\dagger f_{j\sigma} (-1)^j - 2\lambda' \sum_j \left( f_{j\uparrow}^\dagger f_{j\uparrow} + f_{j\downarrow}^\dagger f_{j\downarrow} - 1 \right)^2, \quad (22)$$

and

$$H_{\text{ITF}} = -\chi'_f \sum_{ij} \tau_i^x \tau_j^x + \left( \frac{U}{4} + \lambda' \right) \sum_i \tau_i^z, \quad (23)$$

where the two Hamiltonians are coupled to each other through the following self-consistency equations:

$$\chi_I = \langle \tau_i^x \tau_j^x \rangle, \quad (24)$$

$$\chi'_f = \langle f_{i\sigma}^\dagger f_{j\sigma} \rangle \quad (25)$$

and the Lagrange multiplier  $\lambda'$  is introduced to implement the construct (20) on average. As can be seen, within the present representation, the fermion part, (22) still remains an interacting problem of the Hubbard type, where on-site interaction among the spinons is set by the Lagrange multiplier  $\lambda'$ . The mean field approximation lends itself on the assumption that the system in the enlarged Hilbert space is a product state composed of a spinon part and an Ising part. The spinon part of the wave function is expected have a form close to an Slater determinant and hence the parameter  $\lambda'$  is expected to represent a very small residual interactions between the spinons. Approximate strategies to handle the interacting spinons have been suggested and discussed in Ref. [12]. With this argument we reckon that it is reasonable to assume  $\lambda' = 0$  as an approximate strategy to obtain the simplest possible solution [33].

There are some special lucky situations for the Hubbard model where the partition function  $Z$  happens to be an even function of  $U$ , such as the particle-hole symmetric case considered here [37, 38]. In this case, first of all the Hubbard interaction at half-filling can be written as

$$U n_{j\uparrow} n_{j\downarrow} - \frac{U}{2} (n_{j\uparrow} + n_{j\downarrow}) \quad (26)$$

where due to half-filling condition the chemical potential  $\mu = U/2$  is used and the site index has been dropped for simplicity. Under a particle-hole transformation in one spin sector only (let us call it  $\text{PH}\sigma$  transformation in this paper), namely,

$$c_{j\uparrow}^\dagger = \tilde{c}_{j\uparrow}^\dagger, \quad c_{j\downarrow}^\dagger = (-1)^j \tilde{c}_{j\downarrow}, \quad (27)$$

where  $(-1)^j = \pm 1$  depends on whether it is on sublattice A, or B, the role of charge and spin density are exchanged, namely  $n_\uparrow + n_\downarrow \rightarrow \tilde{n}_\uparrow - \tilde{n}_\downarrow$ . This transformation maps the particle-hole symmetric Hubbard interaction of Eq. (26) to

$$\tilde{U} \tilde{n}_{j\uparrow} \tilde{n}_{j\downarrow} - \frac{\tilde{U}}{2} (\tilde{n}_{j\uparrow} + \tilde{n}_{j\downarrow}) \quad (28)$$

Partial Particle Hole ( $\text{PH}\sigma$ ) transformation					
Before			After		
$\begin{cases} n_\uparrow = 1 \\ n_\downarrow = 0 \end{cases}$	$\uparrow$	$\tau_z = -1$	$\begin{cases} \tilde{n}_\uparrow = 1 \\ \tilde{n}_\downarrow = 1 \end{cases}$	$\uparrow\downarrow$	$\tilde{\tau}_z = -1$
$\begin{cases} n_\uparrow = 0 \\ n_\downarrow = 1 \end{cases}$	$\downarrow$		$\begin{cases} \tilde{n}_\uparrow = 0 \\ \tilde{n}_\downarrow = 0 \end{cases}$	$\circ$	
$\begin{cases} n_\uparrow = 0 \\ n_\downarrow = 0 \end{cases}$	$\circ$	$\tau_z = +1$	$\begin{cases} \tilde{n}_\uparrow = 0 \\ \tilde{n}_\downarrow = 1 \end{cases}$	$\downarrow$	$\tilde{\tau}_z = +1$
$\begin{cases} n_\uparrow = 1 \\ n_\downarrow = 1 \end{cases}$	$\uparrow\downarrow$		$\begin{cases} \tilde{n}_\uparrow = 1 \\ \tilde{n}_\downarrow = 0 \end{cases}$	$\uparrow$	

FIG. 3. (Color online): Schematic summary of partial particle-hole transformation,  $\text{PH}\sigma$  that affects only down-electrons. It basically exchanges the local charge and spin densities. In a setting with one Anderson impurity, the  $\text{PH}\sigma$  would correspond to transformation between spin and charge Kondo effects.

which is nothing but the original Hubbard interaction at half-filling with the only difference that  $\tilde{U} = -U$ . At half-filling under the  $\text{PH}\sigma$  transformation is a symmetry of the Hubbard model which implies properties of system are even with respect to Hubbard  $U$ .

Let us now examine how does the constraint (20) behave under the  $\text{PH}\sigma$  transformation. As indicated in the Fig. 3 the role of  $\text{PH}\sigma$  transformation in terms of Ising spins is to exchange the role of  $|+\rangle$  and  $|-\rangle$  states of Ising variables. Therefore the effect of  $\text{PH}\sigma$  transformation on any operator  $\mathcal{O}$  that contains Ising variables is to change  $\mathcal{O} \rightarrow \tau^x \mathcal{O} \tau^x$ . This transformation leaves the first term in the ITF Hamiltonian (23) intact, but it changes the second term at a given site as

$$\left( \frac{U}{4} + \lambda' \right) \tau^z \rightarrow \left( \frac{U}{4} + \lambda' \right) \tau^x \tau^z \tau^x = - \left( \frac{U}{4} + \lambda' \right) \tau^z = - \left( -\frac{U}{4} + \lambda' \right) \tau^z, \quad (29)$$

where in the last equality we have used the fact that the Hubbard model at half-filling is even with respect to Hubbard  $U$ . This implies that at half-filling for the Hubbard model, the Lagrange multiplier  $\lambda' = 0$ .

Turning on the ionic potential  $(-)^j \Delta (n_\uparrow + n_\downarrow)$ , the  $\text{PH}\sigma$  transformation maps to  $(-)^j \Delta (\tilde{n}_{j\uparrow} - \tilde{n}_{j\downarrow})$ , i.e. the charge density is mapped to spin-density. Therefore the  $\text{PH}\sigma$  is not a symmetry of ionic Hubbard model at half-filling. Hence the partition function has both even and odd parts as a function of  $U$ . This prevents the Lagrange multiplier  $\lambda'$  from becoming zero. However the above symmetry consideration suggests that the physics of ionic (and repulsive) Hubbard model maps onto the physics of attractive Hubbard model in the presence of an staggered magnetization field (since it is couples to spin density in staggered way). Another merit of the above symmetry discussion is that based on the following argument

in Ref. [37], what is precisely missed by *the approximation*  $\lambda' = 0$ : If we slightly deform the constraint (20) to,

$$\mathcal{P}_+ = 1 + \tau_j^z \Omega_j = 0, \quad \Omega_i = 1 - 2(n_j - 1)^2, \quad (30)$$

identifies the operator  $\Omega_j$  to represent the fluctuations of the charge away from half-filling. It was shown in Ref. [37] that to all orders in perturbation theory, the term 1 in  $\mathcal{P}_+$  contributes only in even powers of  $U$  while the second term contributes only in odd powers of  $U$ . Therefore for a half-filled situation of the pure Hubbard model, the effect of second term is nullified, and basically one need not worry about projection. This is another way of saying that the Lagrange multiplier  $\lambda'$  at half-filling becomes zero. By adding ionic term to the half-filled Hubbard model, or placing the Hubbard model itself away from half-filling,  $\lambda'$  is expected to be small based on our earlier argument on small residual interactions. Using the approximation  $\lambda' \approx 0$  in this case amounts to missing the effects that are odd functions of the Hubbard  $U$ .

Within the approximation of  $\lambda' = 0$ , the spinon part describes a non-interacting band of spinons whose bandwidth is renormalized by the  $\chi_I$  parameter obtained from the Ising part. The physics of Mott transition is then captured by the disordering transition of the Ising sector (23) where frozen charge fluctuations are characterized by  $\langle \tau^x \rangle = 0$  [28, 38]. This critical point is essentially equivalent to Brinkman-Rice treatment of the Mott transition [35]. The ordered side of the ITF Hamiltonian (23) is a conducting state: (i) If the underlying rotors are ordered, namely  $\langle e^{i\theta} \rangle \neq 0$  the conducting state within the Hubbard model is a Fermi liquid, while the case  $\langle e^{i\theta} \rangle = 0$  describes the orthogonal metallic state in the Hubbard model. By adding the ionic term  $\Delta$ , it is crucial to note that on-site ionic potential does not couple to neither slave Ising variables, nor to the slave rotor variables. The only effect of the ionic potential  $\Delta$  is to modify the order parameters through the mean field self-consistency equations, but their order-disorder physics remains the same as the Hubbard model. This existence of a region where the Ising variable is ordered, but the rotor variable is disordered endows the non-Mott phase of the ionic Hubbard model with two possible insulating phases: (i) The weak coupling insulator (or Band insulator) where both Ising and rotor are ordered. This can be thought of an underlying ordinary metal that has been gapped out by Bragg reflection of electrons due to sublattice symmetry breaking by the ionic potential. (ii) The intermediate coupling insulator that can be thought of an underlying orthogonal metallic state where the spinons are gapped out by Bragg reflections due to ionic potential. Note that since the spinons within the slave spin representation employed here inherit the charge of electrons, it is natural for them to couple to the staggered electro-static potential  $\Delta$ .

The disordering phase transition of the Ising Hamiltonian (23) can be captured within a simple cluster mean field approximation. Decomposing the lattice to clusters labeled by integer  $I$ , while the sites in a cluster are labeled by integers  $a, b$  etc. Then the Ising variables are denoted by  $\tau_{\Gamma, a}$ . With this re-arrangements, and after mean field decoupling of

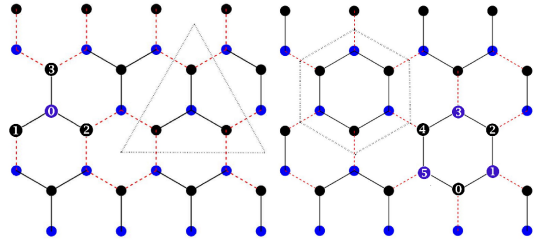


FIG. 4. (Color online) Two choices for the cluster mean field treatment of the slave Ising spins; the Y shaped (left) and hexagonal cluster (right).

the cluster with its surrounding sites via a mean field order parameter  $m = \langle \tau^x \rangle$  (see Fig. 4), the Ising part can be re-written as

$$H = \sum_{\Gamma} H_{\Gamma} \quad (31)$$

where the Hamiltonian for each cluster is,

$$H_{\Gamma} = -\chi'_f \sum_{a, b \in \Gamma} \tau_{\Gamma, a}^x \tau_{\Gamma, b}^x - \frac{mz}{2} \sum_{a \in \Gamma} \tau_{\Gamma, a}^x + \frac{U}{4} \sum_a \tau_{\Gamma, a}^z. \quad (32)$$

In this cluster Hamiltonian, the  $z$  denotes number of bonds crossing the boundary of the cluster. The factor  $1/2$  avoids double counting and  $m = \langle \tau^x \rangle$  is the Ising order parameter that at the mean field level decouples the cluster  $\Gamma$  from its surroundings, but the interactions within the cluster  $\Gamma$  are treated exactly. In Fig. 4 we have depicted clusters used in the present work. For more details on the construction of the Hilbert space and diagonalization of the Hamiltonian, please refer to the Appendix. The Ising disordering considered here for 4-site and 6-site clusters do now show appreciable difference. Therefore in this work we report the critical values  $U_c^{\text{Ising}}$  obtained from 6-site clusters.

## RESULTS

In Fig. 5 we have plotted the results of a slave-rotor mean field for a two-site cluster. The rotor Hilbert space in this plot has been constructed for the angular momentum  $\ell = 2$ . We have checked that the results are not sensitive to increase in the Hilbert space size beyond the  $\ell = 2$ . The left panel shows the evolution of order parameter  $\Phi$  of rotors as a function of Hubbard  $U$  for a selective set of ionic potentials indicated in the legend. As can be seen for  $\Delta = 0$  the critical value  $U_c^{\perp}$  starts around 3.5 and decreases by increasing  $\Delta$ . At  $\Delta = 1$  the critical value for the disordering of single-boson is around 2.8. This means that in the presence of an staggered potential the quasi-particle weight of the underlying metallic bands (to be gapped out by the staggered potential coupled to spinons) is lost at smaller value of  $U$ . The effect of non-zero  $\Delta$  within

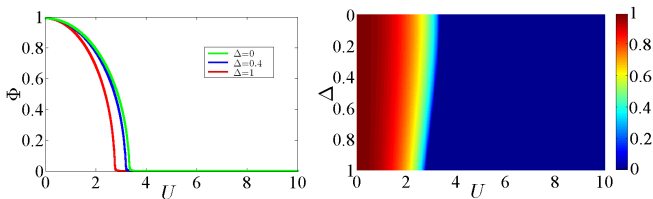


FIG. 5. (Color online) The slave rotor order parameter  $\Phi$ . The right panel shows the intensity plot in the plane of Hubbard  $U$  and ionic potential  $\Delta$  on the honeycomb lattice. The left panel shows the dependence of  $\Phi(U)$  for some selected values of  $\Delta$  as indicated in the legend.

the mean-field self-consistency cycle is assist the Hubbard  $U$  in killing the quasiparticle weight of the underlying metallic state. Right panel in the figure provides an intensity map of the rotor order parameter in the  $(U, \Delta)$  plane. The blue region corresponds to zero single-boson condensation amplitude, and the red corresponds to maximal (i.e. 1) condensation amplitude of single-bosons  $\langle e^{i\theta} \rangle$ .

In Fig. 6 we present the cluster mean field results for the Ising order parameter. The left panel shows the Ising magnetization  $m = \langle \tau^x \rangle$  as a function of  $U$  for selected values of the staggered potential  $\Delta$  indicated in the figure. The right panel provides an intensity map of the Ising order parameter in the  $(U, \Delta)$  plane. The color code is the same as in Fig. 5. By increasing the staggered ionic potential from  $\Delta = 0$  to  $\Delta = 1$ , the critical value  $U_c$  decreases from  $\sim 6.9$  to  $5.7$ . This trend is similar to the behavior of rotor order parameter, i.e. the effort of  $U$  to destroy the Ising order parameter  $m = \langle \tau^x \rangle$  is assisted by the ionic potential  $\Delta$ .

The comparison between the intensity maps in Figs. 5 and 6 shows that there is a clear region between  $U_c^\perp \leq U < U_c$  where the rotor order parameter is zero, i.e. the single boson is not condensed, while the Ising order parameter is non-zero, i.e. the double boson is condensed [28]. In the region  $U < U_c^\perp$  the underlying metallic state has non-zero quasiparticle weight controlled by the rotor order parameter, and vanishes at  $U_c^\perp$ . The spinon sector is gapped out by directly coupling to the staggered potential and therefore the underlying Fermi liquid state becomes a normal band insulator. For

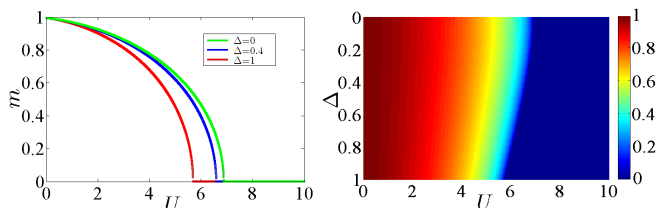


FIG. 6. (Color online) The slave spin order parameter  $m = \langle \tau^x \rangle$ . The right panel shows the intensity plot of the Ising order parameter  $m$  as a function of  $U$  and  $\Delta$ . Right panel shows the variations in the Ising order parameter as a function of  $U$  for some selected values of  $\Delta$  indicated in the legend.

largest values of  $U > U_c$  both the rotor and Ising variables are disordered which prohibit charge fluctuations and the system is a Mott insulator.

For intermediate values of Hubbard  $U_c^\perp \leq U < U_c$  the quasiparticle weight of the underlying Fermi liquid is lost and hence the underlying metallic state has become an orthogonal metal where in the absence of staggered potential the transport would have been done by spinons. However the staggered potential gaps out the underlying non-Fermi liquid (orthogonal metal) state and makes it orthogonal insulator. In this state the states at the bottom of the conduction band and those at the top of the valence band do not carry any quasiparticle weight, and hence the do not couple to ARPES. However, since the current operators is solely constructed by the spinons, the optical conductivity (i.e. the current-current correlation function) does couple to the resulting orthogonal band insulating states. Therefore an important characteristic property of OBI is that the optical conductivity gap is expected to be much smaller than the ARPES gap. For the two-dimensional semiconductors or insulators the ability to tune the chemical potential into the conduction band provides a chance to examine them in ARPES. Once the chemical potential is tuned to the conduction band, the thermally excited carriers into the ARPES-invisible states at the bottom of the conduction band would display quantum oscillations. The downward renormalization of the spinon bandwidth by correlation effects gives an spinon-band effective mass  $\sim 4-5$  times larger than the putative electron-band effective mass. This will in turn be reflected in a corresponding reduction in the cyclotron frequency.

## SUMMARY AND DISCUSSIONS

To summarize, we have investigated the phase transitions of the ionic Hubbard model on the honeycomb lattice using a combination of slave rotor and slave spin mean field theories. The phase diagram of the ionic Hubbard model on the honeycomb lattice within the present method is shown in Fig. 7. For small values of Hubbard  $U < U_c^\perp$  (phase I) we find a normal band insulating (semiconducting) state. For very large values

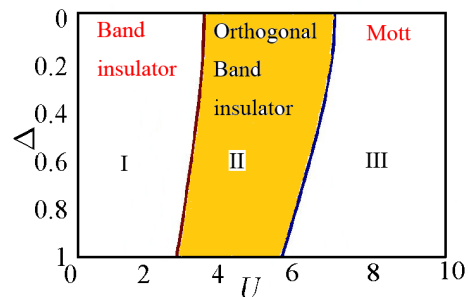


FIG. 7. (Color online): Phase diagram of the ionic Hubbard model within the present combination of slave-rotor and slave-spin methods.

of  $U > U_c$  (phase III) a Mott state is stabilized where neither the rotor order survives ( $\langle e^{i\theta} \rangle = 0$ ), nor Ising order survives ( $\langle \tau^x \rangle = 0$ ). For intermediate values of  $U_c^\perp < U < U_c$  (phase II) we find an exotic orthogonal band insulator where the rotor is disordered,  $\langle e^{i\theta} \rangle = 0$ , but the Ising variables remains ordered,  $\langle \tau^x \rangle \neq 0$ . The exotic nature of this phase lends itself on the chargin pairing [28]. The quasiparticle weight of the physical electrons at the lower critical point,  $U_c^\perp$  vanishes. Since the  $U(1)$  symmetry of the original ionic Hubbard model can not be incorporated into the Ising spins (as they are real matrices), the  $f$  operator inherits the electric charge of electrons and a set of conduction-valence bands of spinons is left for semiconductor transport. Therefore the state II can be viewed as a *spinon semiconductor*.

The essential difference between a phase II orthogonal semiconductor (band insulator) and its normal counterpart is that in a normal band semiconductor (phase I) the band parameters are not much dependent on the temperature. For the orthogonal gapped phases due to the temperature dependence of underlying (slave) Ising order parameter that multiplies the kinetic energy of spinons, the effective mass will correspondingly acquire a temperature dependence characteristic of the Ising order. This can be detected by standard cyclotron resonance experiments and monitoring their temperature dependence  $m^*(T) \sim 1/\langle \tau^x \rangle$ . Particularly when the temperature is high enough to hit the disordering point of the Ising variable  $\langle \tau^x \rangle$  the cyclotron effective mass is expected to diverge in an orthogonal semiconductor. This situation is unlike normal semiconductors where band parameters are almost rigid and do not depend much on the temperature. Another difference behavior appears when the band gap is indirect. In this case a phonon is needed to provide the missing momentum which also provides energy that gives rise to a "tail" of the width  $\omega_D$  (Debye frequency) in the optical absorption. On the other hand the electron phonon interaction  $\sim c_{\vec{k}+\vec{q}}^\dagger c_{\vec{k}} c_{\vec{q}}^\dagger (b_{\vec{q}} + b_{-\vec{q}}^\dagger)$  is directly translated to spinon-phonon coupling  $\langle \tau^x \rangle^2 f_{\vec{k}+\vec{q}}^\dagger f_{\vec{k}} (b_{\vec{q}} + b_{-\vec{q}}^\dagger)$  as the spinons carry the whole  $U(1)$  charge of electrons and hence the optical absorption tail also inherits the temperature dependence of the Ising order parameter. *The temperature dependence of Ising order parameter that is attached to spinons is the key feature of the orthogonal phase.* In normal semiconductors the dominant temperature dependence determining the transport properties appears in the density of excited carriers. However in the orthogonal semiconductor phase, in addition to the carrier density, every property involving the Ising order parameter provides an additional temperature dependence. This can serve not only to distinguish orthogonal semiconductors/insulators from the normal ones, but also as a existence proof for the underlying Ising variable and hence the fractional nature in two-dimensional semiconductors with strong correlations. This example may suggest the correlated semiconductors as alternative rout to search for correlation driven phenomena where the sensitivity of semiconductor carrier density to temperature combined with the temperature dependence of underlying

Ising order parameter help to reveal information about fractional excitation of solids. Furthermore in the absence of tunability of the correlation parameter  $U$  in solids, extra dependence of the underlying Ising order parameter to temperature and magnetic field can serve as conveniently tunable parameters to probe fractional excitations in correlated semiconductors.

The present study addresses the half-filling. Away from half-filling still the orthogonal phase persist [28], but the critical value  $U_c^\perp$  may undergo some quantitative changes. In the case of two-dimensional band insulators where the chemical potential can be easily tuned to conduction band by gating, the ARPES would not be able to reveal the (orthogonal) states near the conduction band minimum (of spinons) as their quasiparticle weight is zero. But since the optical conductivity couples to the electric current that is entirely carried by  $f$  quasiparticles, the optical gap in an OBI is always smaller than the ARPES gap. Furthermore, in a range of energies that would be inside the ARPES gap, cyclotron resonance would give a large effective mass of spinons. The large mass is due to downward renormalization of the spin hopping by the mean field parameter  $\chi_I$ . As pointed out, the characteristic temperature dependence of the underlying Ising condensate determines whether the resonance is due to spinons or electrons.

Within the present mean field approximation thermal probes are coupled to spinons that are *independent* of rotors and Ising spins. The optical probe on the other hand always couples to the above independent spinons in the orthogonal phase. However going beyond the mean field by properly handling the fluctuations of internal gauge fields is expected to provide corrections to the thermal properties as the internal gauge field couples the thermal excitations of spinons to thermal excitations of the rotor and Ising spin. Properly taking the gauge fluctuations into account and its effect on the physical properties of orthogonal states remains to be explored. Thinking along the schematic table of Fig. 1 one may wonder about other possible columns to start with at  $U = 0$ . An interesting possibility can be orthogonal Anderson insulator, where the insulating behavior at  $U = 0$  is due to randomness. This will add another interesting aspect to the Mott-Anderson problem, namely the interplay between the Hubbard  $U$  and randomness around  $U_c^\perp$ , and possible glassy phases of spinons. This problem is currently under investigation in our group [36].

The essential ingredient in a semiconducting or insulating state to push it into the orthogonal phase is the intermediate Coulomb correlations. Possible platforms to search for unusual signature of orthogonal semiconductors would include rare-earth semiconducting systems such as Europium monochalcogenides  $\text{EuX}$  or Samarium monochalcogenides  $\text{SmX}$  where  $\text{X}=\text{S}, \text{Se}, \text{Te}$  [39] and rare earth Nitrides [40]. In particular in the orthogonal phase, an applied magnetic field can directly couple to the Ising order parameter condensate. This may shed light on the observed large magneto-resistance in the monochalcogenides which signals higher sensitivity to applied B-field in these systems as compared to standard s-p semiconductors. Investigation of inhomogeneity and im-

purities in spinon-semiconductors and their contrast normal semiconductors can shed light on exotic properties of semiconducting with spinons. Given the wide use of semiconductors, further exploration of the exotic properties of orthogonal semiconductors may prove useful.

## ACKNOWLEDGEMENTS

We thank A G Moghaddam for useful comments. TF appreciates the Ministry of Science, Research and Technology (MSRT) of Iran for financial support during a visit to Sharif University of Technology.

### Details of exact diagonalization for clusters

In this appendix we present details of the exact diagonalization for the ITF Hamiltonian on a finite cluster for 4 and 6 site clusters. We employ group theory methods to reduce the dimension of ensuing matrices.

#### Y-shaped 4-site cluster

To solve the Eq. (32) first we choose a Y-shaped 4-site cluster  $\Gamma$  shown in Fig. 8. The spin variables at every site have two possible states giving a total of  $2^4 = 16$  possible states for the cluster  $\Gamma$ . Each state of this cluster is of the form  $|\sigma_3, \sigma_2, \sigma_1, \sigma_0\rangle$  where  $\sigma_a$  can take two possible values  $\uparrow, \downarrow$  and the site indices  $a = 0, 1, 2, 3$  are indicated in Fig. 8. The basis in this 16-dimensional Hilbert space are as follows (for brevity we have dropped  $|\rangle$  from the representation of basis states):

$$\begin{aligned} |1\rangle &= \uparrow\uparrow\uparrow\uparrow & |2\rangle &= \uparrow\uparrow\uparrow\downarrow & |3\rangle &= \uparrow\uparrow\downarrow\uparrow & |4\rangle &= \uparrow\downarrow\uparrow\uparrow & (33) \\ |5\rangle &= \downarrow\uparrow\uparrow\uparrow & |6\rangle &= \uparrow\uparrow\downarrow\downarrow & |7\rangle &= \uparrow\downarrow\downarrow\uparrow & |8\rangle &= \downarrow\downarrow\uparrow\uparrow \\ |9\rangle &= \downarrow\uparrow\uparrow\downarrow & |10\rangle &= \uparrow\downarrow\uparrow\downarrow & |11\rangle &= \downarrow\uparrow\downarrow\uparrow & |12\rangle &= \uparrow\downarrow\downarrow\downarrow \\ |13\rangle &= \downarrow\uparrow\downarrow\downarrow & |14\rangle &= \downarrow\downarrow\uparrow\downarrow & |15\rangle &= \downarrow\downarrow\downarrow\uparrow & |16\rangle &= \downarrow\downarrow\downarrow\downarrow \end{aligned}$$

In the 4-site cluster of Fig. 8 the positions 1, 2, 3 are not nearest neighbors of each other, while they are all neighbors of the site 0. So the exchange interaction in the cluster takes place only between the site 0 and the above three sites. Hence the first term of Eq. (32) for the 4-site cluster is,

$$H_1 = - \sum_{\langle a,b \rangle \in \Gamma} \tau_a^x \tau_b^x = - \{ \tau_0^x \tau_1^x + \tau_0^x \tau_2^x + \tau_0^x \tau_3^x \}. \quad (34)$$

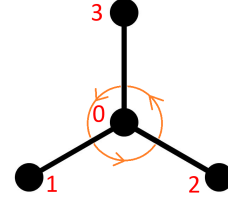


FIG. 8. The Y-shaped 4-site cluster chosen in the exact diagonalization of ITF Hamiltonian. The total Hilbert space of this cluster is  $2^4 = 16$  dimensional labeled by four spins  $|\sigma_0, \sigma_1, \sigma_2, \sigma_3\rangle$  where  $\sigma_i = \uparrow, \downarrow$ .

The effect of the above term on the bases is:

$$\begin{aligned} H_1 |1\rangle &= - \{ |6\rangle + |9\rangle + |10\rangle \} \\ H_1 |2\rangle &= - \{ |3\rangle + |4\rangle + |5\rangle \} \\ H_1 |3\rangle &= - \{ |2\rangle + |12\rangle + |13\rangle \} \\ H_1 |4\rangle &= - \{ |2\rangle + |12\rangle + |14\rangle \} \\ H_1 |5\rangle &= - \{ |2\rangle + |13\rangle + |14\rangle \} \\ H_1 |6\rangle &= - \{ |1\rangle + |7\rangle + |11\rangle \} \\ H_1 |7\rangle &= - \{ |6\rangle + |10\rangle + |16\rangle \} \\ H_1 |8\rangle &= - \{ |9\rangle + |10\rangle + |16\rangle \} \\ H_1 |9\rangle &= - \{ |1\rangle + |8\rangle + |11\rangle \} \\ H_1 |10\rangle &= - \{ |1\rangle + |7\rangle + |8\rangle \} \\ H_1 |11\rangle &= - \{ |6\rangle + |9\rangle + |16\rangle \} \\ H_1 |12\rangle &= - \{ |3\rangle + |4\rangle + |15\rangle \} \\ H_1 |13\rangle &= - \{ |3\rangle + |5\rangle + |15\rangle \} \\ H_1 |14\rangle &= - \{ |4\rangle + |5\rangle + |15\rangle \} \\ H_1 |15\rangle &= - \{ |12\rangle + |13\rangle + |14\rangle \} \\ H_1 |16\rangle &= - \{ |8\rangle + |11\rangle + |12\rangle \}. \end{aligned} \quad (35)$$

The second term of the cluster Hamiltonian (32) is

$$H_2 = - \frac{mz}{2} \sum_{a \in \Gamma} \tau_a^x = - \frac{mz}{2} \{ \tau_0^x + \tau_1^x + \tau_2^x + \tau_3^x \} \quad (36)$$

where  $m$  is the Ising magnetization coupling the boundary sites of the cluster to boundary sites of neighboring clusters and  $z$  is the number of bonds connecting boundary sites 1, 2, 3 to other clusters which for this cluster is  $z = 2$ . The effect of

$H_2$  on the bases is given by,

$$\begin{aligned}
H_2 |1\rangle &= -m \{|2\rangle + |3\rangle + |4\rangle + |5\rangle\} \\
H_2 |2\rangle &= -m \{|1\rangle + |6\rangle + |9\rangle + |10\rangle\} \\
H_2 |3\rangle &= -m \{|1\rangle + |6\rangle + |7\rangle + |11\rangle\} \\
H_2 |4\rangle &= -m \{|1\rangle + |7\rangle + |8\rangle + |10\rangle\} \\
H_2 |5\rangle &= -m \{|1\rangle + |8\rangle + |9\rangle + |11\rangle\} \\
H_2 |6\rangle &= -m \{|2\rangle + |3\rangle + |12\rangle + |13\rangle\} \\
H_2 |7\rangle &= -m \{|3\rangle + |4\rangle + |12\rangle + |15\rangle\} \\
H_2 |8\rangle &= -m \{|4\rangle + |5\rangle + |14\rangle + |15\rangle\} \\
H_2 |9\rangle &= -m \{|2\rangle + |5\rangle + |13\rangle + |14\rangle\} \\
H_2 |10\rangle &= -m \{|2\rangle + |4\rangle + |12\rangle + |14\rangle\} \\
H_2 |11\rangle &= -m \{|3\rangle + |5\rangle + |13\rangle + |15\rangle\} \\
H_2 |12\rangle &= -m \{|6\rangle + |7\rangle + |10\rangle + |16\rangle\} \\
H_2 |13\rangle &= -m \{|6\rangle + |9\rangle + |11\rangle + |16\rangle\} \\
H_2 |14\rangle &= -m \{|8\rangle + |9\rangle + |10\rangle + |16\rangle\} \\
H_2 |15\rangle &= -m \{|7\rangle + |8\rangle + |11\rangle + |16\rangle\} \\
H_2 |16\rangle &= -m \{|12\rangle + |13\rangle + |14\rangle + |15\rangle\}. \quad (37)
\end{aligned}$$

The last term of the cluster Hamiltonian (32) is the transverse field term,

$$H_3 = h \sum_{a \in \Gamma} \tau_a^z = h \{\tau_0^z + \tau_1^z + \tau_2^z + \tau_3^z\}. \quad (38)$$

The above term acts on the 16 bases as follows,

$$\begin{aligned}
H_3 |1\rangle &= 4h |1\rangle, H_3 |2\rangle = 2h |2\rangle \\
H_3 |3\rangle &= 2h |3\rangle, H_3 |4\rangle = 2h |4\rangle \\
H_3 |5\rangle &= 2h |5\rangle \\
H_3 |6\rangle &= 0, H_3 |7\rangle = 0, H_3 |8\rangle = 0 \\
H_3 |9\rangle &= 0, H_3 |10\rangle = 0, H_3 |11\rangle = 0 \\
H_3 |12\rangle &= -2h |12\rangle, H_3 |13\rangle = -2h |13\rangle \\
H_3 |14\rangle &= -2h |14\rangle, H_3 |15\rangle = -2h |15\rangle \\
H_3 |16\rangle &= -4h |16\rangle. \quad (39)
\end{aligned}$$

Let us proceed by employing symmetry considerations to reduce the above 16-dimensional Hamiltonian to smaller blocks. The Y-shaped cluster in Fig. 8 is invariant under rotations by  $2\pi/3$  which is denoted by  $C$  and the group of rotation is formed by  $\{C^0, C^1, C^2\}$ . The effect of this operation on the site labels is

$$C = \begin{cases} 1 \rightarrow 2 \\ 2 \rightarrow 3 \\ 3 \rightarrow 1 \end{cases} \quad (40)$$

Successive operations of  $C$  on a prototypical state, e.g.  $|12\rangle$  gives the following pattern,

$$|12\rangle \xrightarrow{C} |14\rangle \xrightarrow{C} |13\rangle \xrightarrow{C} |12\rangle \quad (41)$$

which is a concise representation of

$$C^0|12\rangle = |12\rangle, C|12\rangle = |14\rangle, C^2|12\rangle = |13\rangle \quad (42)$$

According to projection theorem of group theory a symmetry adopted state in representation labeled by  $n$  can be constructed from an arbitrary state  $|\phi\rangle$  as,

$$|\psi^{(n)}\rangle \sim \left( \sum_g g \Gamma_n[g] \right) |\phi\rangle \quad (43)$$

where  $g$  denotes member of the group, and  $\Gamma_n(g)$  is the  $n$ 'th irreducible representation of element  $g$  of the group. In the case of rotation group the irreducible representations of the cyclic group are labeled by three integer (angular momenta)  $n = 0, \pm 1$  and are represented by  $\{\omega^0, \omega^n, \omega^{2n}\}$  where  $\omega = \exp(2\pi i/3)$ . Compact way of expressing the above representations for the cyclic group is  $\Gamma_n(C^p) = \omega^{pn}$ . This gives a symmetry adopted state build from e.g. basis state  $|12\rangle$  as

$$(C^0 \omega^0 + C^1 \omega^n + C^2 \omega^{2n}) |12\rangle, \quad (44)$$

which after using (42) gives the following state

$$|12\rangle + \omega^n |14\rangle + \omega^{2n} |13\rangle, \quad (45)$$

with definite discrete "angular momentum"  $n$ .

The same symmetry consideration could be applied to every other state which is summarized as,

$$\begin{aligned}
|6\rangle &\xrightarrow{C} |10\rangle \xrightarrow{C} |9\rangle \xrightarrow{C} |6\rangle \\
|3\rangle &\xrightarrow{C} |4\rangle \xrightarrow{C} |5\rangle \xrightarrow{C} |3\rangle \\
|7\rangle &\xrightarrow{C} |8\rangle \xrightarrow{C} |11\rangle \xrightarrow{C} |7\rangle \\
|1\rangle &\xrightarrow{C} |1\rangle, \quad |2\rangle \xrightarrow{C} |2\rangle \\
|15\rangle &\xrightarrow{C} |15\rangle, \quad |16\rangle \xrightarrow{C} |16\rangle. \quad (46)
\end{aligned}$$

Let us now focus on the  $n = +1$  sector. The  $n = -1$  sector has identical spectrum by time-reversal symmetry. The  $n = +1$  sector is spanned by the following normalized states,

$$\begin{aligned}
|\alpha_1\rangle &= \frac{1}{\sqrt{3}} (|12\rangle + \omega |14\rangle + \omega^2 |13\rangle) \\
|\alpha_2\rangle &= \frac{1}{\sqrt{3}} (|3\rangle + \omega |4\rangle + \omega^2 |5\rangle) \\
|\alpha_3\rangle &= \frac{1}{\sqrt{3}} (|6\rangle + \omega |10\rangle + \omega^2 |9\rangle) \\
|\alpha_4\rangle &= \frac{1}{\sqrt{3}} (|7\rangle + \omega |8\rangle + \omega^2 |11\rangle) \quad (47)
\end{aligned}$$

where  $\omega = e^{2i\pi/3}$ . The first term of the cluster Hamiltonian on the above states has the following effect:

$$\begin{aligned}
H_1 |\alpha_1\rangle &= -\Omega_- |\alpha_2\rangle \\
H_1 |\alpha_2\rangle &= -\Omega_+ |\alpha_1\rangle \\
H_1 |\alpha_3\rangle &= -\Omega_+ |\alpha_4\rangle \\
H_1 |\alpha_4\rangle &= -\Omega_- |\alpha_3\rangle \quad (48)
\end{aligned}$$

where  $\Omega_{\pm} = 1 + \omega^{\pm 1} = \exp(\pm i\pi/3)$ . The matrix elements  $\langle \alpha_i | H_1 | \alpha_j \rangle$  are represented in matrix form as,

$$\tilde{H}_1 = - \begin{pmatrix} 0 & \Omega_- & 0 & 0 \\ \Omega_+ & 0 & 0 & 0 \\ 0 & 0 & 0 & \Omega_+ \\ 0 & 0 & \Omega_- & 0 \end{pmatrix} \quad (49)$$

Similarly the  $H_2$  term in this basis becomes,

$$\tilde{H}_2 = -m \begin{pmatrix} 0 & 0 & \Omega_- & 1 \\ 0 & 0 & 1 & \Omega_+ \\ \Omega_+ & 1 & 0 & 0 \\ 1 & \Omega_- & 0 & 0 \end{pmatrix} \quad (50)$$

The transverse field term was already diagonal in the original basis, and remains so in the symmetry adopted basis for the  $n = +1$  sector,

$$\tilde{H}_3 = - \begin{pmatrix} 2h & & & \\ & -2h & & \\ & & 0 & \\ & & & 0 \end{pmatrix} \quad (51)$$

Adding up the above matrices we obtain the matrix representation of the ITF Hamiltonian for Y-shaped cluster in the  $n = +1$  sector as,

$$\tilde{H} = \tilde{H}_1 + \tilde{H}_2 + \tilde{H}_3 = - \begin{pmatrix} 2h & e^{i\pi/3} & me^{i\pi/3} & m \\ e^{-i\pi/3} & -2h & m & me^{-i\pi/3} \\ me^{-i\pi/3} & m & 0 & e^{-i\pi/3} \\ m & me^{i\pi/3} & e^{i\pi/3} & 0 \end{pmatrix} \quad (52)$$

The matrix representation for the  $n = -1$  sector is simply obtained from the above equation by complex conjugation  $i \rightarrow -i$  corresponding to time reversal operation. The matrix representation in the  $n = 0$  sector can be constructed in similar way. The ground state is the least eigen-value among all sectors with various  $n$  values. Here it turns out that the ground state belongs to  $n = 0$  sector.

### Hexagonal cluster

The details of the group theory consideration for larger clusters is similar to Y-shaped cluster. In this section for reference we only provide explicit representation of all  $2^6 = 64$  basis states and the effects of cluster ITF Hamiltonian on it. As can be seen in Fig. 2 each hexagonal cluster  $\Gamma$  is connected to the rest of the lattice by  $z = 1$  neighbor. The basis is labeled as before by  $|\sigma_5, \sigma_4, \sigma_3, \sigma_2, \sigma_1, \sigma_0\rangle$  where the site index  $a$  in  $\sigma_a$  varies from 0 to 5 as depicted in right panel of Fig. 2.

$$\begin{aligned} |1\rangle &= \downarrow\downarrow\downarrow\downarrow\downarrow & |2\rangle &= \downarrow\downarrow\downarrow\downarrow\uparrow & |3\rangle &= \downarrow\downarrow\downarrow\uparrow\downarrow & |4\rangle &= \downarrow\downarrow\downarrow\uparrow\uparrow \\ |5\rangle &= \downarrow\downarrow\uparrow\downarrow\downarrow & |6\rangle &= \downarrow\downarrow\uparrow\uparrow\downarrow & |7\rangle &= \downarrow\downarrow\uparrow\uparrow\downarrow & |8\rangle &= \downarrow\downarrow\uparrow\uparrow\uparrow \\ |9\rangle &= \downarrow\downarrow\uparrow\downarrow\downarrow & |10\rangle &= \downarrow\downarrow\uparrow\downarrow\uparrow & |11\rangle &= \downarrow\downarrow\uparrow\downarrow\downarrow & |12\rangle &= \downarrow\downarrow\uparrow\downarrow\uparrow \\ |13\rangle &= \downarrow\downarrow\uparrow\uparrow\downarrow & |14\rangle &= \downarrow\downarrow\uparrow\uparrow\uparrow & |15\rangle &= \downarrow\downarrow\uparrow\uparrow\downarrow & |16\rangle &= \downarrow\downarrow\uparrow\uparrow\uparrow \\ |17\rangle &= \downarrow\uparrow\downarrow\downarrow\downarrow & |18\rangle &= \downarrow\uparrow\downarrow\downarrow\uparrow & |19\rangle &= \downarrow\uparrow\downarrow\downarrow\downarrow & |20\rangle &= \downarrow\uparrow\downarrow\downarrow\uparrow \\ |21\rangle &= \downarrow\uparrow\downarrow\uparrow\downarrow & |22\rangle &= \downarrow\uparrow\downarrow\uparrow\uparrow & |23\rangle &= \downarrow\uparrow\downarrow\uparrow\downarrow & |24\rangle &= \downarrow\uparrow\downarrow\uparrow\uparrow \\ |25\rangle &= \downarrow\uparrow\uparrow\downarrow\downarrow & |26\rangle &= \downarrow\uparrow\uparrow\downarrow\uparrow & |27\rangle &= \downarrow\uparrow\uparrow\downarrow\downarrow & |28\rangle &= \downarrow\uparrow\uparrow\downarrow\uparrow \\ |29\rangle &= \downarrow\uparrow\uparrow\uparrow\downarrow & |30\rangle &= \downarrow\uparrow\uparrow\uparrow\uparrow & |31\rangle &= \downarrow\uparrow\uparrow\uparrow\downarrow & |32\rangle &= \downarrow\uparrow\uparrow\uparrow\uparrow \\ |33\rangle &= \uparrow\downarrow\downarrow\downarrow\downarrow & |34\rangle &= \uparrow\downarrow\downarrow\downarrow\uparrow & |35\rangle &= \uparrow\downarrow\downarrow\downarrow\downarrow & |36\rangle &= \uparrow\downarrow\downarrow\downarrow\uparrow \\ |37\rangle &= \uparrow\downarrow\downarrow\uparrow\downarrow & |38\rangle &= \uparrow\downarrow\downarrow\uparrow\uparrow & |39\rangle &= \uparrow\downarrow\downarrow\uparrow\downarrow & |40\rangle &= \uparrow\downarrow\downarrow\uparrow\uparrow \\ |41\rangle &= \uparrow\downarrow\uparrow\downarrow\downarrow & |42\rangle &= \uparrow\downarrow\uparrow\downarrow\uparrow & |43\rangle &= \uparrow\downarrow\uparrow\downarrow\downarrow & |44\rangle &= \uparrow\downarrow\uparrow\downarrow\uparrow \\ |45\rangle &= \uparrow\downarrow\uparrow\uparrow\downarrow & |46\rangle &= \uparrow\downarrow\uparrow\uparrow\uparrow & |47\rangle &= \uparrow\downarrow\uparrow\uparrow\downarrow & |48\rangle &= \uparrow\downarrow\uparrow\uparrow\uparrow \\ |49\rangle &= \uparrow\uparrow\downarrow\downarrow\downarrow & |50\rangle &= \uparrow\uparrow\downarrow\downarrow\uparrow & |51\rangle &= \uparrow\uparrow\downarrow\downarrow\downarrow & |52\rangle &= \uparrow\uparrow\downarrow\downarrow\uparrow \\ |53\rangle &= \uparrow\uparrow\downarrow\uparrow\downarrow & |54\rangle &= \uparrow\uparrow\downarrow\uparrow\uparrow & |55\rangle &= \uparrow\uparrow\downarrow\uparrow\downarrow & |56\rangle &= \uparrow\uparrow\downarrow\uparrow\uparrow \\ |57\rangle &= \uparrow\uparrow\uparrow\downarrow\downarrow & |58\rangle &= \uparrow\uparrow\uparrow\downarrow\uparrow & |59\rangle &= \uparrow\uparrow\uparrow\downarrow\downarrow & |60\rangle &= \uparrow\uparrow\uparrow\downarrow\uparrow \\ |61\rangle &= \uparrow\uparrow\uparrow\uparrow\downarrow & |62\rangle &= \uparrow\uparrow\uparrow\uparrow\uparrow & |63\rangle &= \uparrow\uparrow\uparrow\uparrow\downarrow & |64\rangle &= \uparrow\uparrow\uparrow\uparrow\uparrow \end{aligned} \quad (53)$$

the first term of Eq. (32) for 6-site cluster is,

$$H_1 = - \sum_{(a,b) \in \Gamma} \tau_a^x \tau_b^x \quad (54)$$

$$= - (\tau_0^x \tau_1^x + \tau_1^x \tau_2^x + \tau_2^x \tau_3^x + \tau_3^x \tau_4^x + \tau_4^x \tau_5^x + \tau_5^x \tau_0^x).$$

The effect of the above term on the 64-basis states is,

$$\begin{aligned} H_1 |1\rangle &= - \{|4\rangle + |7\rangle + |13\rangle + |25\rangle + |34\rangle + |49\rangle\} \\ H_1 |2\rangle &= - \{|3\rangle + |8\rangle + |14\rangle + |26\rangle + |33\rangle + |50\rangle\} \\ H_1 |3\rangle &= - \{|2\rangle + |5\rangle + |15\rangle + |27\rangle + |36\rangle + |51\rangle\} \\ H_1 |4\rangle &= - \{|1\rangle + |6\rangle + |16\rangle + |28\rangle + |35\rangle + |52\rangle\} \\ H_1 |5\rangle &= - \{|8\rangle + |3\rangle + |9\rangle + |29\rangle + |38\rangle + |53\rangle\} \\ H_1 |6\rangle &= - \{|7\rangle + |4\rangle + |10\rangle + |30\rangle + |37\rangle + |54\rangle\} \\ H_1 |7\rangle &= - \{|6\rangle + |1\rangle + |11\rangle + |31\rangle + |40\rangle + |55\rangle\} \\ H_1 |8\rangle &= - \{|5\rangle + |2\rangle + |12\rangle + |32\rangle + |39\rangle + |56\rangle\} \\ H_1 |9\rangle &= - \{|12\rangle + |15\rangle + |5\rangle + |17\rangle + |42\rangle + |57\rangle\} \\ H_1 |10\rangle &= - \{|11\rangle + |16\rangle + |6\rangle + |18\rangle + |41\rangle + |58\rangle\} \\ H_1 |11\rangle &= - \{|10\rangle + |13\rangle + |7\rangle + |19\rangle + |44\rangle + |59\rangle\} \\ H_1 |12\rangle &= - \{|9\rangle + |14\rangle + |8\rangle + |20\rangle + |43\rangle + |60\rangle\} \\ H_1 |13\rangle &= - \{|16\rangle + |11\rangle + |1\rangle + |21\rangle + |46\rangle + |61\rangle\} \\ H_1 |14\rangle &= - \{|15\rangle + |12\rangle + |2\rangle + |22\rangle + |45\rangle + |62\rangle\} \\ H_1 |15\rangle &= - \{|14\rangle + |9\rangle + |3\rangle + |23\rangle + |48\rangle + |63\rangle\} \\ H_1 |16\rangle &= - \{|13\rangle + |10\rangle + |4\rangle + |24\rangle + |47\rangle + |64\rangle\} \\ H_1 |17\rangle &= - \{|20\rangle + |23\rangle + |29\rangle + |9\rangle + |50\rangle + |33\rangle\} \\ H_1 |18\rangle &= - \{|19\rangle + |24\rangle + |30\rangle + |10\rangle + |49\rangle + |34\rangle\} \\ H_1 |19\rangle &= - \{|18\rangle + |21\rangle + |31\rangle + |11\rangle + |52\rangle + |35\rangle\} \\ H_1 |20\rangle &= - \{|17\rangle + |22\rangle + |32\rangle + |12\rangle + |51\rangle + |36\rangle\} \end{aligned}$$

$$\begin{aligned}
H_1 |21\rangle &= -\{|24\rangle + |19\rangle + |25\rangle + |13\rangle + |54\rangle + |37\rangle\} \\
H_1 |22\rangle &= -\{|23\rangle + |20\rangle + |26\rangle + |14\rangle + |53\rangle + |38\rangle\} \\
H_1 |23\rangle &= -\{|22\rangle + |17\rangle + |27\rangle + |15\rangle + |56\rangle + |39\rangle\} \\
H_1 |24\rangle &= -\{|21\rangle + |18\rangle + |28\rangle + |16\rangle + |55\rangle + |40\rangle\} \\
H_1 |25\rangle &= -\{|28\rangle + |15\rangle + |21\rangle + |1\rangle + |58\rangle + |41\rangle\} \\
H_1 |26\rangle &= -\{|27\rangle + |16\rangle + |22\rangle + |2\rangle + |57\rangle + |42\rangle\} \\
H_1 |27\rangle &= -\{|26\rangle + |29\rangle + |23\rangle + |3\rangle + |60\rangle + |43\rangle\} \\
H_1 |28\rangle &= -\{|25\rangle + |30\rangle + |24\rangle + |4\rangle + |59\rangle + |44\rangle\} \\
H_1 |29\rangle &= -\{|32\rangle + |27\rangle + |17\rangle + |5\rangle + |62\rangle + |45\rangle\} \\
H_1 |30\rangle &= -\{|31\rangle + |28\rangle + |18\rangle + |6\rangle + |61\rangle + |46\rangle\}
\end{aligned}$$

$$\begin{aligned}
H_1 |31\rangle &= -\{|30\rangle + |25\rangle + |19\rangle + |7\rangle + |64\rangle + |47\rangle\} \\
H_1 |32\rangle &= -\{|29\rangle + |26\rangle + |20\rangle + |8\rangle + |63\rangle + |48\rangle\} \\
H_1 |33\rangle &= -\{|36\rangle + |39\rangle + |45\rangle + |57\rangle + |2\rangle + |17\rangle\} \\
H_1 |34\rangle &= -\{|35\rangle + |40\rangle + |46\rangle + |58\rangle + |1\rangle + |18\rangle\} \\
H_1 |35\rangle &= -\{|34\rangle + |37\rangle + |47\rangle + |59\rangle + |4\rangle + |19\rangle\} \\
H_1 |36\rangle &= -\{|33\rangle + |38\rangle + |48\rangle + |60\rangle + |3\rangle + |20\rangle\} \\
H_1 |37\rangle &= -\{|40\rangle + |35\rangle + |41\rangle + |61\rangle + |6\rangle + |21\rangle\} \\
H_1 |38\rangle &= -\{|39\rangle + |36\rangle + |42\rangle + |62\rangle + |5\rangle + |22\rangle\} \\
H_1 |39\rangle &= -\{|38\rangle + |33\rangle + |43\rangle + |63\rangle + |8\rangle + |23\rangle\} \\
H_1 |40\rangle &= -\{|37\rangle + |34\rangle + |44\rangle + |64\rangle + |7\rangle + |24\rangle\}
\end{aligned}$$

$$\begin{aligned}
H_1 |41\rangle &= -\{|44\rangle + |47\rangle + |37\rangle + |49\rangle + |10\rangle + |25\rangle\} \\
H_1 |42\rangle &= -\{|43\rangle + |48\rangle + |38\rangle + |50\rangle + |9\rangle + |26\rangle\} \\
H_1 |43\rangle &= -\{|42\rangle + |45\rangle + |39\rangle + |51\rangle + |12\rangle + |27\rangle\} \\
H_1 |44\rangle &= -\{|41\rangle + |46\rangle + |40\rangle + |52\rangle + |11\rangle + |28\rangle\} \\
H_1 |45\rangle &= -\{|48\rangle + |43\rangle + |33\rangle + |53\rangle + |14\rangle + |29\rangle\} \\
H_1 |46\rangle &= -\{|47\rangle + |44\rangle + |34\rangle + |54\rangle + |13\rangle + |30\rangle\} \\
H_1 |47\rangle &= -\{|46\rangle + |41\rangle + |35\rangle + |55\rangle + |16\rangle + |31\rangle\} \\
H_1 |48\rangle &= -\{|45\rangle + |42\rangle + |36\rangle + |56\rangle + |15\rangle + |32\rangle\} \\
H_1 |49\rangle &= -\{|52\rangle + |55\rangle + |61\rangle + |41\rangle + |18\rangle + |1\rangle\} \\
H_1 |50\rangle &= -\{|51\rangle + |56\rangle + |62\rangle + |42\rangle + |17\rangle + |2\rangle\}
\end{aligned}$$

$$\begin{aligned}
H_1 |51\rangle &= -\{|50\rangle + |53\rangle + |63\rangle + |43\rangle + |20\rangle + |3\rangle\} \\
H_1 |52\rangle &= -\{|49\rangle + |54\rangle + |64\rangle + |44\rangle + |19\rangle + |4\rangle\} \\
H_1 |53\rangle &= -\{|56\rangle + |51\rangle + |57\rangle + |45\rangle + |22\rangle + |5\rangle\} \\
H_1 |54\rangle &= -\{|55\rangle + |52\rangle + |58\rangle + |46\rangle + |21\rangle + |6\rangle\} \\
H_1 |55\rangle &= -\{|54\rangle + |49\rangle + |59\rangle + |47\rangle + |24\rangle + |7\rangle\} \\
H_1 |56\rangle &= -\{|53\rangle + |50\rangle + |60\rangle + |48\rangle + |23\rangle + |8\rangle\} \\
H_1 |57\rangle &= -\{|60\rangle + |63\rangle + |53\rangle + |33\rangle + |26\rangle + |9\rangle\} \\
H_1 |58\rangle &= -\{|59\rangle + |64\rangle + |54\rangle + |34\rangle + |25\rangle + |10\rangle\} \\
H_1 |59\rangle &= -\{|58\rangle + |61\rangle + |55\rangle + |35\rangle + |28\rangle + |11\rangle\} \\
H_1 |60\rangle &= -\{|57\rangle + |62\rangle + |56\rangle + |36\rangle + |27\rangle + |12\rangle\}
\end{aligned}$$

$$\begin{aligned}
H_1 |61\rangle &= -\{|64\rangle + |59\rangle + |49\rangle + |37\rangle + |30\rangle + |13\rangle\} \\
H_1 |62\rangle &= -\{|63\rangle + |60\rangle + |50\rangle + |38\rangle + |29\rangle + |14\rangle\} \\
H_1 |63\rangle &= -\{|62\rangle + |57\rangle + |51\rangle + |39\rangle + |32\rangle + |15\rangle\} \\
H_1 |64\rangle &= -\{|61\rangle + |58\rangle + |52\rangle + |40\rangle + |31\rangle + |16\rangle\}
\end{aligned} \tag{55}$$

The second term of the cluster Hamiltonian (32) is

$$H_2 = -\frac{m}{2} \{\tau_0^x + \tau_1^x + \tau_2^x + \tau_3^x + \tau_4^x + \tau_5^x\} \tag{56}$$

for the above equation the number of bonds connecting to other clusters is  $z = 1$ . The effect of  $H_2$  on the basis is given by:

$$\begin{aligned}
H_2 |1\rangle &= \frac{-m}{2} \{|2\rangle + |3\rangle + |5\rangle + |9\rangle + |17\rangle + |33\rangle\} \\
H_2 |2\rangle &= \frac{-m}{2} \{|1\rangle + |4\rangle + |6\rangle + |10\rangle + |18\rangle + |34\rangle\} \\
H_2 |3\rangle &= \frac{-m}{2} \{|4\rangle + |1\rangle + |7\rangle + |11\rangle + |19\rangle + |35\rangle\} \\
H_2 |4\rangle &= \frac{-m}{2} \{|3\rangle + |2\rangle + |8\rangle + |12\rangle + |20\rangle + |36\rangle\} \\
H_2 |5\rangle &= \frac{-m}{2} \{|6\rangle + |7\rangle + |1\rangle + |13\rangle + |21\rangle + |37\rangle\} \\
H_2 |6\rangle &= \frac{-m}{2} \{|5\rangle + |8\rangle + |2\rangle + |14\rangle + |22\rangle + |38\rangle\} \\
H_2 |7\rangle &= \frac{-m}{2} \{|8\rangle + |5\rangle + |3\rangle + |15\rangle + |23\rangle + |39\rangle\} \\
H_2 |8\rangle &= \frac{-m}{2} \{|7\rangle + |6\rangle + |4\rangle + |16\rangle + |24\rangle + |40\rangle\} \\
H_2 |9\rangle &= \frac{-m}{2} \{|10\rangle + |11\rangle + |13\rangle + |1\rangle + |25\rangle + |41\rangle\} \\
H_2 |10\rangle &= \frac{-m}{2} \{|9\rangle + |12\rangle + |14\rangle + |2\rangle + |26\rangle + |42\rangle\} \\
H_2 |11\rangle &= \frac{-m}{2} \{|12\rangle + |9\rangle + |15\rangle + |3\rangle + |27\rangle + |43\rangle\} \\
H_2 |12\rangle &= \frac{-m}{2} \{|11\rangle + |10\rangle + |16\rangle + |4\rangle + |28\rangle + |44\rangle\} \\
H_2 |13\rangle &= \frac{-m}{2} \{|14\rangle + |15\rangle + |9\rangle + |5\rangle + |29\rangle + |45\rangle\} \\
H_2 |14\rangle &= \frac{-m}{2} \{|13\rangle + |16\rangle + |10\rangle + |6\rangle + |30\rangle + |46\rangle\} \\
H_2 |15\rangle &= \frac{-m}{2} \{|16\rangle + |13\rangle + |11\rangle + |7\rangle + |31\rangle + |47\rangle\} \\
H_2 |16\rangle &= \frac{-m}{2} \{|15\rangle + |14\rangle + |12\rangle + |8\rangle + |32\rangle + |48\rangle\} \\
H_2 |17\rangle &= \frac{-m}{2} \{|18\rangle + |19\rangle + |21\rangle + |25\rangle + |1\rangle + |49\rangle\} \\
H_2 |18\rangle &= \frac{-m}{2} \{|17\rangle + |20\rangle + |22\rangle + |26\rangle + |2\rangle + |50\rangle\} \\
H_2 |19\rangle &= \frac{-m}{2} \{|20\rangle + |17\rangle + |23\rangle + |27\rangle + |3\rangle + |51\rangle\} \\
H_2 |20\rangle &= \frac{-m}{2} \{|19\rangle + |18\rangle + |24\rangle + |28\rangle + |4\rangle + |52\rangle\}
\end{aligned}$$

$$\begin{aligned}
H_2 |21\rangle &= \frac{-m}{2} \{|22\rangle + |23\rangle + |17\rangle + |29\rangle + |5\rangle + |53\rangle\} \\
H_2 |22\rangle &= \frac{-m}{2} \{|21\rangle + |24\rangle + |18\rangle + |30\rangle + |6\rangle + |54\rangle\} \\
H_2 |23\rangle &= \frac{-m}{2} \{|24\rangle + |21\rangle + |19\rangle + |31\rangle + |7\rangle + |55\rangle\} \\
H_2 |24\rangle &= \frac{-m}{2} \{|23\rangle + |22\rangle + |20\rangle + |32\rangle + |8\rangle + |56\rangle\} \\
H_2 |25\rangle &= \frac{-m}{2} \{|26\rangle + |27\rangle + |29\rangle + |17\rangle + |9\rangle + |57\rangle\} \\
H_2 |26\rangle &= \frac{-m}{2} \{|25\rangle + |28\rangle + |30\rangle + |18\rangle + |10\rangle + |58\rangle\} \\
H_2 |27\rangle &= \frac{-m}{2} \{|28\rangle + |25\rangle + |31\rangle + |19\rangle + |11\rangle + |59\rangle\} \\
H_2 |28\rangle &= \frac{-m}{2} \{|27\rangle + |26\rangle + |32\rangle + |20\rangle + |12\rangle + |60\rangle\} \\
H_2 |29\rangle &= \frac{-m}{2} \{|30\rangle + |31\rangle + |25\rangle + |21\rangle + |13\rangle + |61\rangle\} \\
H_2 |30\rangle &= \frac{-m}{2} \{|29\rangle + |32\rangle + |26\rangle + |22\rangle + |14\rangle + |62\rangle\}
\end{aligned}$$

$$\begin{aligned}
H_2 |31\rangle &= \frac{-m}{2} \{|32\rangle + |29\rangle + |27\rangle + |23\rangle + |15\rangle + |63\rangle\} \\
H_2 |32\rangle &= \frac{-m}{2} \{|31\rangle + |30\rangle + |28\rangle + |24\rangle + |16\rangle + |64\rangle\} \\
H_2 |33\rangle &= \frac{-m}{2} \{|34\rangle + |35\rangle + |37\rangle + |41\rangle + |49\rangle + |1\rangle\} \\
H_2 |34\rangle &= \frac{-m}{2} \{|33\rangle + |36\rangle + |38\rangle + |42\rangle + |50\rangle + |2\rangle\} \\
H_2 |35\rangle &= \frac{-m}{2} \{|36\rangle + |33\rangle + |39\rangle + |43\rangle + |51\rangle + |3\rangle\} \\
H_2 |36\rangle &= \frac{-m}{2} \{|35\rangle + |34\rangle + |40\rangle + |44\rangle + |52\rangle + |4\rangle\} \\
H_2 |37\rangle &= \frac{-m}{2} \{|38\rangle + |39\rangle + |33\rangle + |45\rangle + |53\rangle + |5\rangle\} \\
H_2 |38\rangle &= \frac{-m}{2} \{|37\rangle + |40\rangle + |34\rangle + |46\rangle + |54\rangle + |6\rangle\} \\
H_2 |39\rangle &= \frac{-m}{2} \{|40\rangle + |37\rangle + |35\rangle + |47\rangle + |55\rangle + |7\rangle\} \\
H_2 |40\rangle &= \frac{-m}{2} \{|39\rangle + |38\rangle + |36\rangle + |48\rangle + |56\rangle + |8\rangle\}
\end{aligned}$$

$$\begin{aligned}
H_2 |41\rangle &= \frac{-m}{2} \{|42\rangle + |43\rangle + |45\rangle + |49\rangle + |57\rangle + |9\rangle\} \\
H_2 |42\rangle &= \frac{-m}{2} \{|41\rangle + |44\rangle + |46\rangle + |34\rangle + |58\rangle + |10\rangle\} \\
H_2 |43\rangle &= \frac{-m}{2} \{|44\rangle + |41\rangle + |47\rangle + |35\rangle + |59\rangle + |11\rangle\} \\
H_2 |44\rangle &= \frac{-m}{2} \{|43\rangle + |42\rangle + |48\rangle + |36\rangle + |60\rangle + |12\rangle\} \\
H_2 |45\rangle &= \frac{-m}{2} \{|46\rangle + |47\rangle + |41\rangle + |37\rangle + |61\rangle + |13\rangle\} \\
H_2 |46\rangle &= \frac{-m}{2} \{|45\rangle + |48\rangle + |42\rangle + |38\rangle + |62\rangle + |14\rangle\} \\
H_2 |47\rangle &= \frac{-m}{2} \{|48\rangle + |45\rangle + |43\rangle + |39\rangle + |63\rangle + |15\rangle\} \\
H_2 |48\rangle &= \frac{-m}{2} \{|47\rangle + |46\rangle + |44\rangle + |40\rangle + |64\rangle + |16\rangle\} \\
H_2 |49\rangle &= \frac{-m}{2} \{|50\rangle + |51\rangle + |53\rangle + |57\rangle + |33\rangle + |17\rangle\} \\
H_2 |50\rangle &= \frac{-m}{2} \{|49\rangle + |52\rangle + |54\rangle + |58\rangle + |34\rangle + |18\rangle\}
\end{aligned}$$

$$\begin{aligned}
H_2 |51\rangle &= \frac{-m}{2} \{|52\rangle + |49\rangle + |55\rangle + |59\rangle + |35\rangle + |19\rangle\} \\
H_2 |52\rangle &= \frac{-m}{2} \{|51\rangle + |50\rangle + |56\rangle + |60\rangle + |36\rangle + |20\rangle\} \\
H_2 |53\rangle &= \frac{-m}{2} \{|54\rangle + |55\rangle + |49\rangle + |61\rangle + |37\rangle + |21\rangle\} \\
H_2 |54\rangle &= \frac{-m}{2} \{|53\rangle + |56\rangle + |50\rangle + |62\rangle + |38\rangle + |22\rangle\} \\
H_2 |55\rangle &= \frac{-m}{2} \{|56\rangle + |53\rangle + |51\rangle + |63\rangle + |39\rangle + |23\rangle\} \\
H_2 |56\rangle &= \frac{-m}{2} \{|55\rangle + |54\rangle + |52\rangle + |64\rangle + |40\rangle + |24\rangle\} \\
H_2 |57\rangle &= \frac{-m}{2} \{|58\rangle + |59\rangle + |61\rangle + |49\rangle + |41\rangle + |25\rangle\} \\
H_2 |58\rangle &= \frac{-m}{2} \{|57\rangle + |60\rangle + |62\rangle + |50\rangle + |42\rangle + |26\rangle\} \\
H_2 |59\rangle &= \frac{-m}{2} \{|60\rangle + |57\rangle + |63\rangle + |51\rangle + |43\rangle + |27\rangle\} \\
H_2 |60\rangle &= \frac{-m}{2} \{|59\rangle + |58\rangle + |64\rangle + |52\rangle + |44\rangle + |28\rangle\} \\
H_2 |61\rangle &= \frac{-m}{2} \{|62\rangle + |63\rangle + |57\rangle + |53\rangle + |45\rangle + |29\rangle\} \\
H_2 |62\rangle &= \frac{-m}{2} \{|61\rangle + |64\rangle + |58\rangle + |54\rangle + |46\rangle + |30\rangle\} \\
H_2 |63\rangle &= \frac{-m}{2} \{|64\rangle + |61\rangle + |59\rangle + |55\rangle + |47\rangle + |31\rangle\} \\
H_2 |64\rangle &= \frac{-m}{2} \{|63\rangle + |62\rangle + |60\rangle + |56\rangle + |48\rangle + |32\rangle\}
\end{aligned} \tag{57}$$

Finally the last term of the cluster Hamiltonian (32) is the transverse field term,

$$H_3 = h \{\tau_0^z \tau_1^z + \tau_2^z + \tau_3^z + \tau_4^z + \tau_5^z\} \tag{58}$$

The effect of above term on the 64 bases is:

$$\begin{aligned}
H_3 |1\rangle &= -6h |1\rangle, & H_3 |2\rangle &= -4h |2\rangle, \\
H_3 |3\rangle &= -4h |3\rangle, & H_3 |4\rangle &= -2h |4\rangle, \\
H_3 |5\rangle &= -4h |5\rangle, & H_3 |6\rangle &= -2h |6\rangle, \\
H_3 |7\rangle &= -4h |7\rangle, & H_3 |8\rangle &= 0, \\
H_3 |9\rangle &= -4h |9\rangle, & H_3 |10\rangle &= -2h |10\rangle, \\
H_3 |11\rangle &= -2h |11\rangle, & H_3 |12\rangle &= 0, \\
H_3 |13\rangle &= -2h |13\rangle, & H_3 |14\rangle &= 0, \\
H_3 |15\rangle &= 0, & H_3 |16\rangle &= 2h |16\rangle, \\
H_3 |17\rangle &= -4h |17\rangle, & H_3 |18\rangle &= -2h |18\rangle, \\
H_3 |19\rangle &= -2h |19\rangle, & H_3 |20\rangle &= 0, \\
H_3 |21\rangle &= -2h |21\rangle, & H_3 |22\rangle &= 0, \\
H_3 |23\rangle &= 0, & H_3 |24\rangle &= 2h |24\rangle, \\
H_3 |25\rangle &= -2h |25\rangle, & H_3 |26\rangle &= 0, \\
H_3 |27\rangle &= 0, & H_3 |28\rangle &= 2h |28\rangle, \\
H_3 |29\rangle &= 0, & H_3 |30\rangle &= 2h |30\rangle, \\
H_3 |31\rangle &= 2h |31\rangle, & H_3 |32\rangle &= 4h |32\rangle, \\
H_3 |33\rangle &= -4h |33\rangle, & H_3 |34\rangle &= -2h |34\rangle, \\
H_3 |35\rangle &= -2h |35\rangle, & H_3 |36\rangle &= 0, \\
H_3 |37\rangle &= -2h |37\rangle, & H_3 |38\rangle &= 0, \\
H_3 |39\rangle &= 0, & H_3 |40\rangle &= 2h |40\rangle, \\
H_3 |41\rangle &= -2h |41\rangle, & H_3 |42\rangle &= 0, \\
H_3 |43\rangle &= 0, & H_3 |44\rangle &= 2h |44\rangle, \\
H_3 |45\rangle &= 0, & H_3 |46\rangle &= 2h |46\rangle, \\
H_3 |47\rangle &= 2h |47\rangle, & H_3 |48\rangle &= 4h |48\rangle, \\
H_3 |49\rangle &= -2h |49\rangle, & H_3 |50\rangle &= 0, \\
H_3 |51\rangle &= 0, & H_3 |52\rangle &= 2h |52\rangle, \\
H_3 |53\rangle &= 0, & H_3 |54\rangle &= 2h |54\rangle, \\
H_3 |55\rangle &= 2h |55\rangle, & H_3 |56\rangle &= 4h |56\rangle, \\
H_3 |57\rangle &= 0, & H_3 |58\rangle &= 2h |58\rangle, \\
H_3 |59\rangle &= 2h |59\rangle, & H_3 |60\rangle &= 4h |60\rangle, \\
H_3 |61\rangle &= 2h |61\rangle, & H_3 |62\rangle &= 4h |62\rangle, \\
H_3 |63\rangle &= 4h |63\rangle, & H_3 |64\rangle &= 6h |64\rangle. \quad (59)
\end{aligned}$$

The above  $64 \times 64$  Hamiltonian can be diagonalized on computer even without resort to group theory methods.

---

\* akbar.jafari@gmail.com

- [1] S. N. Mott *Metal-Insulator Transitions* (Taylor and Francis, London, 1990)
- [2] M. Imada, A. Fujimori, Y. Tokura, Rev. Mod. Phys. (1998) **70**, 1039.
- [3] M. C. Gutzwiller, Phys. Rev. (1965) **137**, A1726.
- [4] P. Edegger, V. M. Muthukumar, C. Gros, Adv. Phys. (2007) **56** 927.
- [5] W. Metzner, Phys. Rev. B (1990) **43**, 8549.
- [6] S. Pairault, D. Snychal, and A.-M. S. Tremblay, Phys. Rev. Lett.(1998) **80**,5389; S. Pairault, D. S en echal and A.-M. S. Tremblay, Eur. Phys. J. B (2000) **16**, 85.
- [7] E. Adibi, S. A. Jafari arXiv:1509.09076v1 (2015), to appear in Phys. Rev. B (2016)
- [8] M. I. Vladimirov, V. A. Moskalenko, Theor. Math. Phys. (1990) **82**, 301; *ibid* (1990) **85**, 1185.
- [9] S. G. Ovchinnikov, V. V. Val'kov, *Hubbard operators in the theory of strongly correlated electrons* (Imperial College Press, 2004).
- [10] P. A. Lee, N. Nagaosa, X. G. Wen, Rev. Mod. Phys. (2006) **78**, 17.
- [11] S. Florens, A. Georges, Phys. Rev. B (2004) **70**, 035114.
- [12] A. Regg, S. D. Huber, and M. Sigrist, Phys. Rev. B (2010) **81**, 155118.
- [13] S. R. Hassan and L. de Medici, Phys. Rev. B (2010) **81**, 035106.
- [14] T. Tohyama, Y. Inoue, K. Tsutsui, and S. Maekawa, Phys. Rev. B (2005) **72**, 045113.
- [15] E. Dagotto, Rev. Mod. Phys. (1994) **66**, 763.
- [16] S. Sorella, E. Tosatti, EPL (Europhysics Letters) (1992) **19** 699.
- [17] T. Kashima, M. Imada, J. Phys. Soc. Jpn. (2001) **70**, 2287.
- [18] A. Georges, G. Kotliar, W. Krauth, and M. J. Rozenberg Rev. Mod. Phys.(1996) **68**, 13; G. Kotliar, S. Y. Savrasov, K. Haule, V. S. Oudovenko, O. Parcollet, and C. A. Marianetti Rev. Mod. Phys. (2006) **78**, 865.
- [19] T. Egami, S. Ishihara, M. Tachiki, Science (1993) **261**, 1307.
- [20] M. Fabrizio, A.O. Gogolin, A.A. Nersisyan, Phys. Rev. Lett. (1999) **83**, 2014.
- [21] M. Hafez-Torbati, G. Uhrig, arXiv:1509.04996 (2015).
- [22] D. Prychynenko, S. D. Huber, Physica B (2016) **481** 53.
- [23] A. Garg, H. R. Krishnamurthy, M. Randeria, Phys. Rev. Lett. (2006) **97** 046403.
- [24] M. Hafez, S. A. Jafari, M. R. Abolhassani, Phys. Lett. A (2009) **373** 4479; M. Hafez, S. A. Jafari, Sh. Adibi, F. Shahbazi, Phys. Rev. B (2010) **81** 245131.
- [25] K. Bouadim, N. Paris, F. Hebert, G. G. Batrouni, and R. T. Scalettar, Phys. Rev. B (2007) **76** 085112,
- [26] M. Ebrahimkhas, S. A. Jafari, Euro. Phys. Lett. (2012) **98** 27009.
- [27] R. K. Kaul, Physics (2012) **5** 82.
- [28] R. Nandkishore, M. A. Metlitski, and T. Senthil Phys. Rev. B (2012) **86**, 045128.
- [29] Y. Zhong, K. Liu, Y. Q. Wang, H. G. Luo Phys. Rev. B (2012) **86**, 165134.
- [30] S. Florens and A. Georges, Phys. Rev. B (2002) **66** 165111.
- [31] E. Zhao, A. Paramekanti, Phys. Rev. B (2007) **76** 195101.
- [32] R. Yu, Q. Si, Phys. Rev. B (2011) **84** 235115.
- [33] A. Rüegg, G. A. Fiete, Phys. Rev. Lett. (2012) **108** 046401.
- [34] M. S. Nevius, M. Conrad, F. Wang, A. Celis, M. N. Nair, A. Taleb Ibrahim, A. Tejada and E. H. Conrad, Phys. Rev. Lett. (2015) **115** 136802.
- [35] S. Sachdev *Quantum phase transitions* (Wiley Online Library, 2007); D. Vollhardt, Rev. Mod. Phys. (1984) **56** 99.
- [36] M. Amini, S. A. Jafari (in progress)
- [37] M. Schiro, M. Fabrizio, Phys. Rev. B (2011) **83** 165105.
- [38] R. Zitko, M. Fabrizio, Phys. Rev. B (2015) **91** 245130.
- [39] I. A. Smirnov, Sov. Phys. Uspek., (1976) **19** 1034.
- [40] N. Sclar, J. App. Phys. (1962) **33** 2999; N. Sclar *ibid*, (1964) **35** 1534.